REPORT

Final Report

Development and Proof Testing of Basic Technology Needed for High-Temperature Operation of $LiBr/H_2O$ for Absorption Chiller Cycles

To

Martin Marietta Energy Systems, Inc.

March 31, 1995

Battelle
. . . Putting Technology To Work

FINAL REPORT

DEVELOPMENT AND PROOF TESTING OF BASIC TECHNOLOGY NEEDED FOR HIGH-TEMPERATURE OPERATION OF $LiBr/H_2O$ FOR ABSORPTION CHILLER CYCLES

March 31, 1995

to

Martin Marietta Energy Systems, Inc.

from

Battelle
. . . Putting Technology To Work

505 King Avenue
Columbus, Ohio 43201-2693

Summary

This report summarizes the results and efforts on the project "Development and Proof Testing of Basic Technology Needed for High-Temperature Operation of $LiBr/H_20$ for Absorption Chiller Cycles." Two areas of basic technology were investigated in this project: the use of solution additives to enhance absorber performance in a high-temperature chiller cycle, and the identification of a set of materials of construction, corrosion inhibitors, and performance additives that can withstand the corrosive effects of $LiBr/H_2O$ solutions at temperatures up to 450°F.

These areas of technology are important to the development of triple-effect chillers using only $LiBr/H_2O$ as their working fluids. Such chillers offer the potential for higher efficiency and lower energy consumption than double-effect chillers, but they require a peak generator temperature that is expected to be in the 400 to 500°F range.

Conventional chillers use an additive, an octyl alcohol (2-ethyl-1-hexanol, or 2EH), to improve mass transfer in the absorber. This additive begins to decompose at a high rate at temperatures above 350°F. Efforts to identify other additives that could better withstand the 450°F temperatures expected in a triple-effect cycle were partially successful. High-temperature additives were found that improved absorber performance in basic tests, but none of these new additives was as effective as an octyl alcohol. Hence, there was a need to identify ways of separating the octyl alcohol from the solution stream leaving the absorber.

Conventional corrosion inhibitors and materials of construction had not previously been studied at such high temperatures because the peak temperature in double-effect cycles is only about 330°F. Furthermore, there was a need to evaluate corrosion

inhibitors that did not involve the use of chromates, since the use of chromates leads to concerns about disposal of hazardous materials when a chiller is decharged.

In the area of absorber additives, the goal was to design, build, and test components and subsystems for the separation of conventional additives from a flowing stream of solution to minimize the potential decomposition of the additive in a high-temperature generator. In the area of materials compatibility, the objective was to identify and evaluate up to three potential corrosion inhibitors for use at temperatures in the 400 to 500°F range that allow the use of cost-effective materials of construction in a triple-effect chiller.

The approach for achieving the additive separation objective was to identify and screen alternative technologies for separating the absorber additive from the solution, evaluate the best candidates in bench-scale experiments, and test the best of these in full-scale chiller tests. A brief scoping analysis was also conducted to illustrate the sensitivity of additive concentration to the additive separation efficiency. Finally, a test was conducted to show the effectiveness of one of the more promising alternative additives in an actual chiller test. The approach for achieving the materials compatibility objective was to conduct a series of materials/inhibitor tests using sample coupons, leading to the selection of the most promising low-cost alternatives, and the evaluation of these in dedicated, closed-loop tests. These closed-loop tests provided information on the gas generation rate for the material/ inhibitor combinations of interest and information on the physical response of the combination to two-phase flow conditions.

The additive separation efforts on this project did not lead to the identification of an apparently attractive means to separate 2EH from the solution, thereby minimizing its decomposition and allowing its use to enhance absorber performance in a chiller having a generator operating temperature in the 400 to 500°F range. The separations tests completed in this project led to the conclusion that additives like 2EH probably cannot be economically

separated from the solution by using gravimetric, thermal, or electroacoustic techniques. The best alternatives may be

- To use only additives with high-temperature stability,
- To continue to use 2EH (octyl alcohol) as the absorber additive and replenish it as needed, or
- To identify and develop another separation technique.

A stable, high-temperature additive was tested in the absorber of a 40 RT chiller. These tests showed a technically significant improvement in absorber performance, but the improvement was significantly less than can be obtained with 2EH.

The materials-compatibility efforts on this project showed the potential for using both a molybdate and a silicate as independent corrosion inhibitors in 450 to 500°F LiBr solutions. Weight-loss coupon tests showed that some lower cost alloys might resist the corrosive attack of the LiBr solution well enough to be of practical value. However, corrosion loop tests involving similar alloys showed high initial gas generation rates, especially when compared to purge-system capacities that typify small-scale (3 to 100 RT) chillers. It is anticipated that the corrosion rates implied by the measured high gas generation rates in the corrosion loop tests may require the reevaluation of the materials choices for a high-temperature chiller. A cupro-nickel alloy was tested in one of the corrosion loops as a heat-exchanger material. Although this alloy cannot contribute to the gas generation rate, it may not be acceptable in a chiller because of copper precipitation issues. Copper has been known to precipitate from LiBr solutions and plate-out on solution pump parts, leading to pump failures. One such occurrence took place during the corrosion loop tests on this project.

Table of Contents

Page

Summary iii

Nomenclature List x

Introduction 1
- Objective 2
- Approach 3

Results 4
- Absorber Additive Evaluations 4
  - Background 4
  - Separator Evaluations 5
  - Alternative Additive Test 17
- Materials Compatibility Evaluations 19
  - Background 19
  - Electrochemical Coupon Testing 20
  - Weight-Loss Coupon Testing 23
  - Additional Coupon Tests 35
  - Results of the Additional Coupon Tests 39
  - Corrosion Loop Tests 45
    - Corrosion Loop Construction 51
    - Testing Results 53

Conclusions 59
- Additive Separation Evaluations 59
- Materials Compatibility Evaluations 60
- Materials Recommendations 61
  - Generator Materials 61
  - Heat Exchanger Materials 62

List of Tables

Table 1. Results of Full Scale Separation Tests in a 40 RT Chiller 14

Table 2. List of Alloys Tested in Electrochemical Tests, Their SAE Class, and Their Composition 22

List of Tables, Continued

Table 3. Inhibitor Formulations 22

Table 4. List of Alloys Tested in Weight-Loss Tests, Their SAE Class, and Their Composition 27

Table 5. Coupon Test Matrix for Addition Weight-Loss Tests 37

Table 6. Alloy List for Additional Weight-Loss Tests 40

Table 7. Corrosion Loop Materials Test Matrix 49

List of Figures

Figure 1. Schematic diagram of an idealized separator and chiller 7

Figure 2. Results of one model calculation showing additive concentration as a function of time (full separator flow to generator) 9

Figure 3. Summary of model predictions (10-minute residence time in separators) . . . 10

Figure 4. Detail drawing of separation chambers 11

Figure 5. Elevation drawing of separation chambers, as installed 12

Figure 6. Schematic diagram of separation system and 40 RT chiller 13

Figure 7. Additive concentration at the absorber exit during an extended test 16

Figure 8. Wilson plot for additive tests in a 40 RT chiller 18

Figure 9. Electrochemical polarization test schematic 23

Figure 10. Idealized polarization test results 24

Figure 11. Polarization test results for alloy C1018 at 450°F 25

Figure 12. Polarization test results for alloy 2205 at 450°F 26

Figure 13. Corrosion rate results for chromate inhibitor at 450°F for 32 days, fully immersed flat coupons 28

Figure 14. Corrosion rate results for molybdate inhibitor at 450°F for 32 and 64 days, fully immersed flat coupons 29

Figure 15. Corrosion rate results for silicate inhibitor at 450°F for 32 days, fully immersed flat coupons 30

Figure 16. Corrosion rate results for chromate inhibitor at 450°F for 32 days — partially immersed flat coupons 33

Figure 17. Corrosion rate results for silicate inhibitor at 450°F for 32 days — partially immersed flat coupons 34

Figure 18. Corrosion rate results for three hydroxide concentrations in silicate-inhibited solutions at 450°F, fully immersed flat coupons, except as noted 41

Figure 19. Corrosion rate results in silicate inhibited solutions at 450°F, fully immersed flat coupons 42

Figure 20. Corrosion rate results in silicate-inhibited solutions at 500°F, fully immersed flat coupons 43

Figure 21. Corrosion rate results in silicate inhibited solutions at 500°F with four chloride concentrations, teardrop coupons, partially immersed 44

Figure 22. Corrosion rate results in molybdate inhibited solutions with and without sulfate, fully immersed flat coupons 46

Figure 23. Corrosion rate results in molybdate inhibited solutions at 475°F, fully immersed flat coupons 47

Figure 24. Corrosion rate results in molybdate inhibited solutions at 500°F, fully immersed flat coupons 48

Figure 25. Schematic diagram for the corrosion test loops 52

Figure 26. Gas generation rate for loop 1, F11 generator and SA 179 heat exchanger 54

Figure 27. Gas generation rate for loop 2, 410 generator and SA 179 heat exchanger 55

Figure 28. Gas generation rate for loop 3, A-109 generator and 90Cu-10Ni heat exchanger 56

Nomenclature List

delta E pit	Potential difference for pitting-mv
e	Electron flow
E	Impressed electrochemical potential-mv
I	Current-ma
LiBr	Lithium Bromide salt
m	Mass flow rate-lb/min
ma	Current-milliamperes
mv	Potential-millivolts
SCE	Saturated Calomel Electrode
U	Overall heat-transfer coefficient-Btu/hr-ft^2-°F
x	Concentration

FINAL REPORT

DEVELOPMENT AND PROOF TESTING OF BASIC TECHNOLOGY NEEDED FOR HIGH-TEMPERATURE OPERATION OF $LiBr/H_2O$ FOR ABSORPTION CHILLER CYCLES

to

Martin Marietta Energy Systems, Inc.

from

Battelle

March 31, 1995

Introduction

This report summarizes the results and efforts on the project "Development and Proof Testing of Basic Technology Needed for High-Temperature Operation of $LiBr/H_2O$ for Absorption Chiller Cycles." Two areas of basic technology were investigated in this project:

1. Use of solution additives to enhance absorber performance in a high-temperature chiller cycle

2. Identification of a set of materials of construction, corrosion inhibitor, and performance additives that can withstand the corrosive effects of $LiBr/H_2O$ solutions at temperatures up to 450°F.

These areas of technology are important to the development of triple-effect chillers using only $LiBr/H_2O$ as their working fluids. Such chillers offer the potential for

higher efficiency and lower energy consumption than double-effect chillers, but they require a peak generator temperature that is expected to be in the 400 to 500°F range.

Conventional chillers use an additive, an octyl alcohol (2-ethyl-1-hexanol, or 2EH), to improve mass transfer in the absorber. However, as discussed later, this additive begins to decompose at a high rate at temperatures above 350°F. Efforts to identify other additives that could better withstand the 450°F temperatures expected in a triple-effect cycle were partially successful. High-temperature additives were found that improved absorber performance in basic tests, but none of these new additives was as effective as an octyl alcohol. Hence, there was a need to identify ways of separating the octyl alcohol from the solution stream leaving the absorber. An efficient separation scheme would allow the use of the octyl alcohol additive without exposing it to the high temperature of the primary generator.

In addition, conventional corrosion inhibitors, such as chromates and molybdates, and materials of construction, such as carbon steel and copper, had not been evaluated at such high temperatures because the peak temperature in a double-effect cycles is only about 330°F. Further, because the use of chromates leads to concerns about disposal of hazardous materials when a chiller is decharged, there was a need to evaluate corrosion inhibitors that did not involve the use of chromates. Thus, there was a need to identify corrosion inhibitors and construction materials for high-temperature (450°F) operation.

Objective

The overall objective of the project was the development and proof testing of the basic technology needed to operate with $LiBr/H_20$ at the higher temperatures needed for advanced absorption chiller cycles. The subobjectives for the project were defined as

1. To reduce to practice the operation of $LiBr/H_20$ absorption fluids and to identify problems associated with higher temperature operation.

2. To establish the upper temperature limit which is practical with $LiBr/H_20$ absorption fluids using molybdate inhibitors.

3. To establish methods of "dynamic concentration control" for $LiBr/H_20$ absorption fluids using lithium molybdate (or approved substitute) corrosion inhibitors and to establish an upper temperature for their use.

4. To develop methods and techniques to allow the use of conventional heat-and-mass transfer additives at the higher temperatures without excessive thermal decomposition.

5. To establish other combinations of corrosion inhibitors, heat-and-mass transfer additives, material pretreatments and/or materials of construction which will allow $LiBr/H_20$ operation at the higher temperatures if lithium molybdate or the standard additives can not adequately operate at higher temperatures.

Approach

The approach toward the additive separation objectives was to identify and screen alternative technologies for separating the absorber additive from the solution, evaluate the best candidates in bench-scale experiments, and test the best of these in full-scale chiller tests. A brief scoping analysis was also conducted to illustrate the sensitivity of additive concentration to the additive separation efficiency. Finally, a test was conducted to show the effectiveness of one of the more promising alternative additives in an actual chiller test.

The approach toward the materials compatibility objectives was to conduct a series of materials/inhibitor tests using sample coupons, leading to the selection of the most promising low-cost alternatives, and the evaluation of these in dedicated, closed-loop tests. These closed-loop tests provided information on the gas generation rate for the material/inhibitor combinations of interest and information on the physical response of the material/inhibitor combinations to two-phase flow conditions.

Results

Absorber Additive Evaluations

Background

An important part of this project was the evaluation of ways to enhance the performance of the absorber in a high-temperature chiller. In most chillers the solution contains an organic additive to enhance heat and, especially, mass transfer in the absorber. Reiner* at ORNL has shown that the best additives for enhancing absorber performance will break down if they are exposed to the temperatures expected in the generator of a high-temperature chiller. Hence, one of the tasks in this project was to evaluate ways of separating an additive from the solution stream that enters the generator.

By separating the additive from the solution flow going to the generator, one can prevent or retard the decomposition of an additive that will break down at the higher generator temperatures (400 to 500°F) envisioned for a high-temperature chiller. Tests at ORNL (Reiner, et.al) showed that one specific octyl alcohol, 2 ethyl hexanol (2EH), decomposes at about 200 C (392°F), which is well below the 450°F generator temperature expected in a chiller using the Dual Condenser Coupled (DCC) cycle. A basic assumption of the additive evaluations is that a system is needed that allows enough additive to survive in the chiller long enough that the additive replacement is cost-effective. Note that complete separation should not be expected, nor is complete separation needed for a practical chiller. A further part of this assumption is that the breakdown products of the additive are removed from the chiller before they can interfere with the chiller's operation in any way, hence there is no special focus on purge systems to specifically remove additive decomposition products.

---

* Reiner, R.H., W. Del Cul, A. Zaltash, and H. Perez-Blanco, *Evaluation of Potential Performance Additives for the Advanced LiBr Chiller*, ORNL/CON-318.

Separator Evaluations

Techniques for separating two liquids were reviewed to identify potential separation means for evaluation. The review identified only a few techniques that appeared to be both simple and potentially effective. Separation of the 2EH additive was known to occur due to poor mixing of solution in chillers, so the consideration of a settling chamber appeared to be reasonable. Also, the 2EH additive was known to vaporize in the generator of a chiller, so a reboiler, or distillation chamber, offered promise, but with one limitation. That limitation is that the boiling of the additive from the solution requires heating all the solution and results in some vaporization of refrigerant water. Thus, the heat input to boil the additive is significant relative to the net heat input to the chiller and the resulting vapor is a mixture of 2EH and water in the vapor state. The subsequent separation of the 2EH and water could be accomplished by a distillation process such as is done in the rectifier section of an ammonia/water chiller. A new technique to electroacoustically separate the two liquids was briefly considered and evaluated, but the LiBr solution was too highly conductive (electrically) for this method to be practical.

Two bench-scale separators were tested: a simple settling chamber and a reboiler. Both chambers gave a significant (20 to 60 percent separation efficiency) separation effect, but neither chamber gave complete separation. A "full-scale" settling chamber was also tested on a double-effect chiller, with the finding that significant, but inadequate separation occurred.

The bench-scale settling chamber consisted of a clear plastic tank having an overflow weir near one end. Solution was pumped into the other end of the chamber and allowed to drift toward the weir. Part of the flow was withdrawn from the bottom of the chamber, near the weir, and the remainder of the solution flowed over the weir. Samples of the three solution flows were taken and the flow rates were measured, so the separation efficiency could be calculated. Separation efficiencies of 20 to 60 percent were measured. Separation efficiency increased when the solution flow rate was reduced, increasing the

residence time for the solution in the settling chamber. The best results were obtained with residence times of 10 to 20 minutes, giving the basis for designing the full-size settling chambers for the 40 RT chiller.

These relatively long residence time results required that the settling chamber for the chiller be large and contain a significant volume of solution. Although the settling chamber might be an inexpensive component to construct and install on a chiller, there were two other issues of concern. One was the added weight of the solution in the settling chamber and the other issue was the cost of this solution.

Cost estimates were made that showed, for a 400 RT capacity chiller using 2EH as the additive, a maximum savings in materials cost of about $2,000. The savings were assumed to be the materials cost of the additional 30 percent of the absorber tubes needed if an additive is not used. As a point of reference, the separation chamber actually tested on the 40RT chiller was about 75 percent efficient, at best, and required 180 gallons of extra solution at about $37/gal. Thus, for a 400 RT chiller, the extra solution required (materials cost) for this (inadequate) separator would be over $6,600. Clearly, this is not acceptable on a materials cost basis.

Given the potential for high costs for the solution to charge a settling chamber and the measured separation efficiency of the bench-scale chamber, it was decided to conduct a limiting case analysis to estimate the lifetime of an additive charge for various assumed separation efficiencies. This analysis was conducted late in the design effort for the full-scale settling chamber. Figure 1 shows a schematic diagram of the ideal separation system considered in this analysis. The separation system is characterized by the assumed separation efficiency that is an input to the model. A further assumption (worst-case scenario) is that all the additive not recovered in the separator is destroyed in the generator. The model also includes the presence of a bypass flow from the exit of the separation chamber back to the absorber. This flow is present in the basic chiller used in the tests, and is typically 50 percent of the flow rate leaving the absorber. The model calculates the operating time for the

ADDITIVE DESTRUCTION CALCULATION

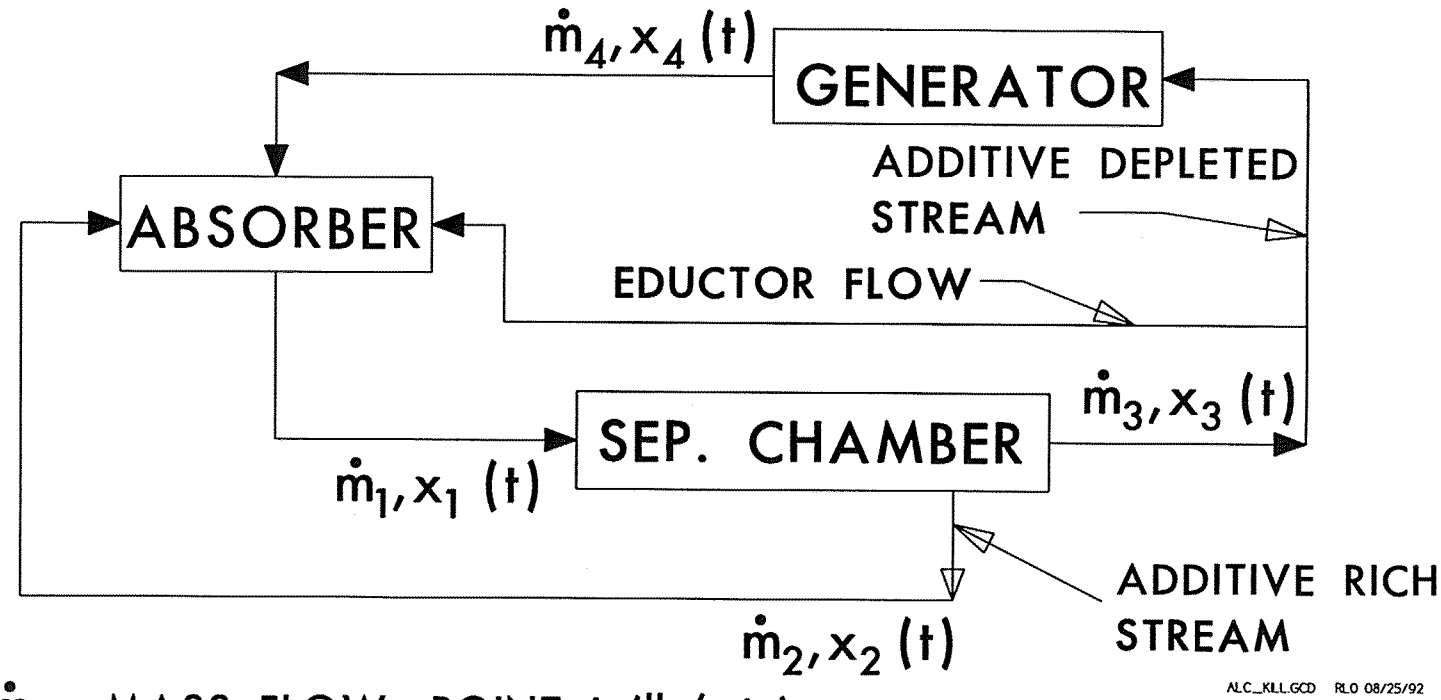

$\dot{m}_i$ = MASS FLOW, POINT i (lb/min)

x_i = ADDITIVE CONCENTRATION, POINT i (ppm)

Figure 1. Schematic diagram of an idealized separator and chiller

chiller and separator before the specified initial charge of additive is reduced to any given concentration in the solution.

Figure 2 shows the results from a typical analysis. These results show that the initial charge of additive (typically 20,000 ppm in the test chiller) is depleted at a decreasing rate for 30 operating days before the concentration is reduced to less than that needed for effective absorber performance. Figure 3 summarizes the results for several model calculations. These results indicate that a separation system will have to exceed 99 percent efficiency (perhaps up to 99.99 percent) to yield acceptable additive life between rechargings. If such high efficiencies are indeed needed, it will be difficult to achieve a cost-effective separation system using settling chambers, because of the high cost of the large solution inventory needed.

Full-scale separator tests were conducted using the 40 RT chiller and the chambers shown in Figures 4 and 5. These chambers were designed using the results of the bench-scale test chambers, scaled-up to the flow rate for the chiller. Figure 4 shows the details of each chamber. Figure 5 shows how both chambers were installed below the chiller. Solution leaving the absorber flowed through both chambers in series. Hence, the second chamber had a reduced solution flow rate and additive concentration. Figure 6 shows the schematic arrangement of the flow through the separation chambers and the location of the sampling points.

The Table 1 shows the results from four key tests of the separation system, with one column of data for each test (1 to 4). The first column gives the sample point designation, as shown on Figure 6. The second column designates the key variables for each sample point. Two variables were measured at each point for each test, the 2EH concentration and the solution flow rate. The 2EH flow rate is the product of the two measured variables. The 2EH concentration was measured by taking a solution sample and using an off-line chemical technique. The chemical technique was calibrated using prepared samples of known 2EH concentration. The separation efficiency is one minus the ratio of additive flow rates at

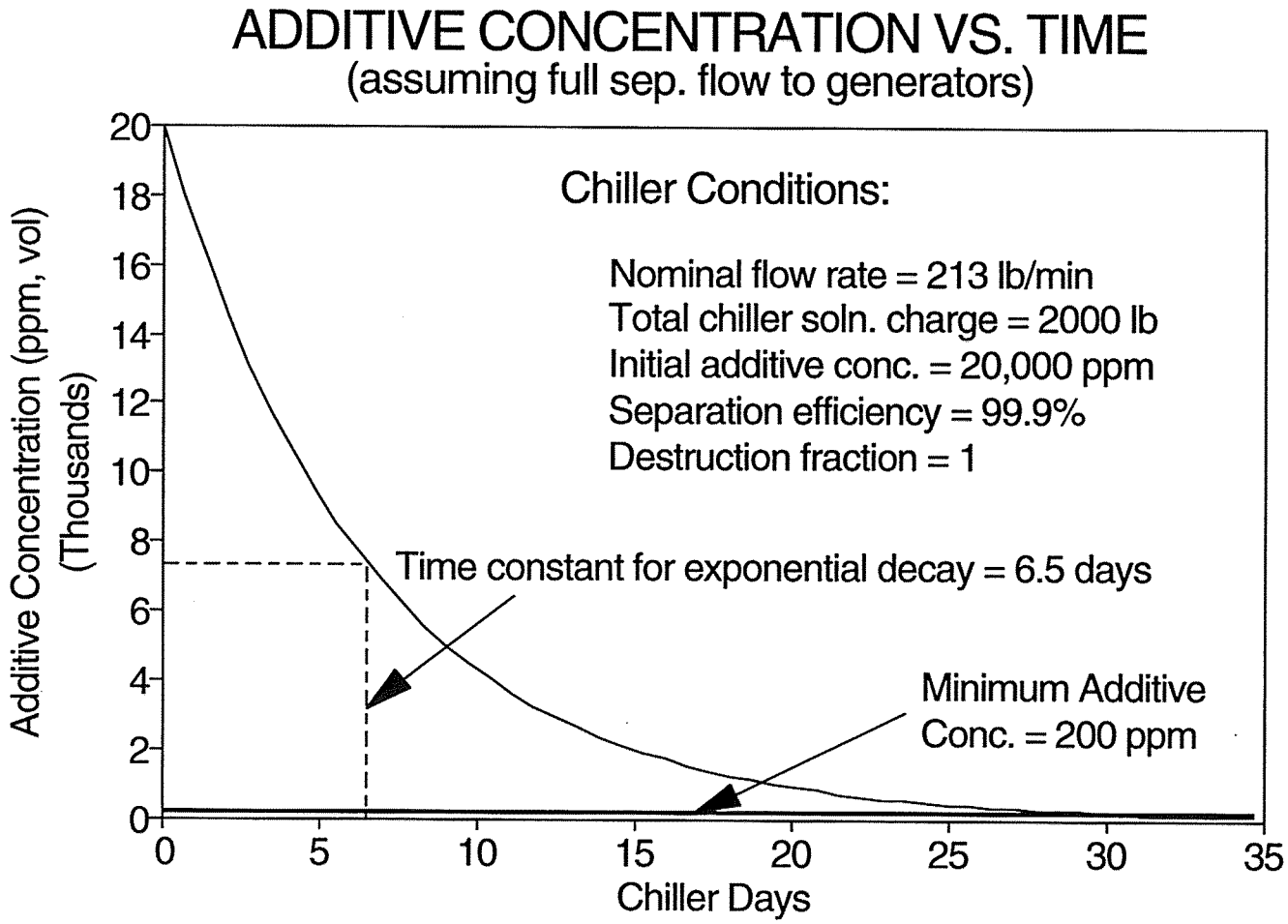

Figure 2. **Results of one model calculation showing additive concentration as a function of time (full separator flow to generator)**

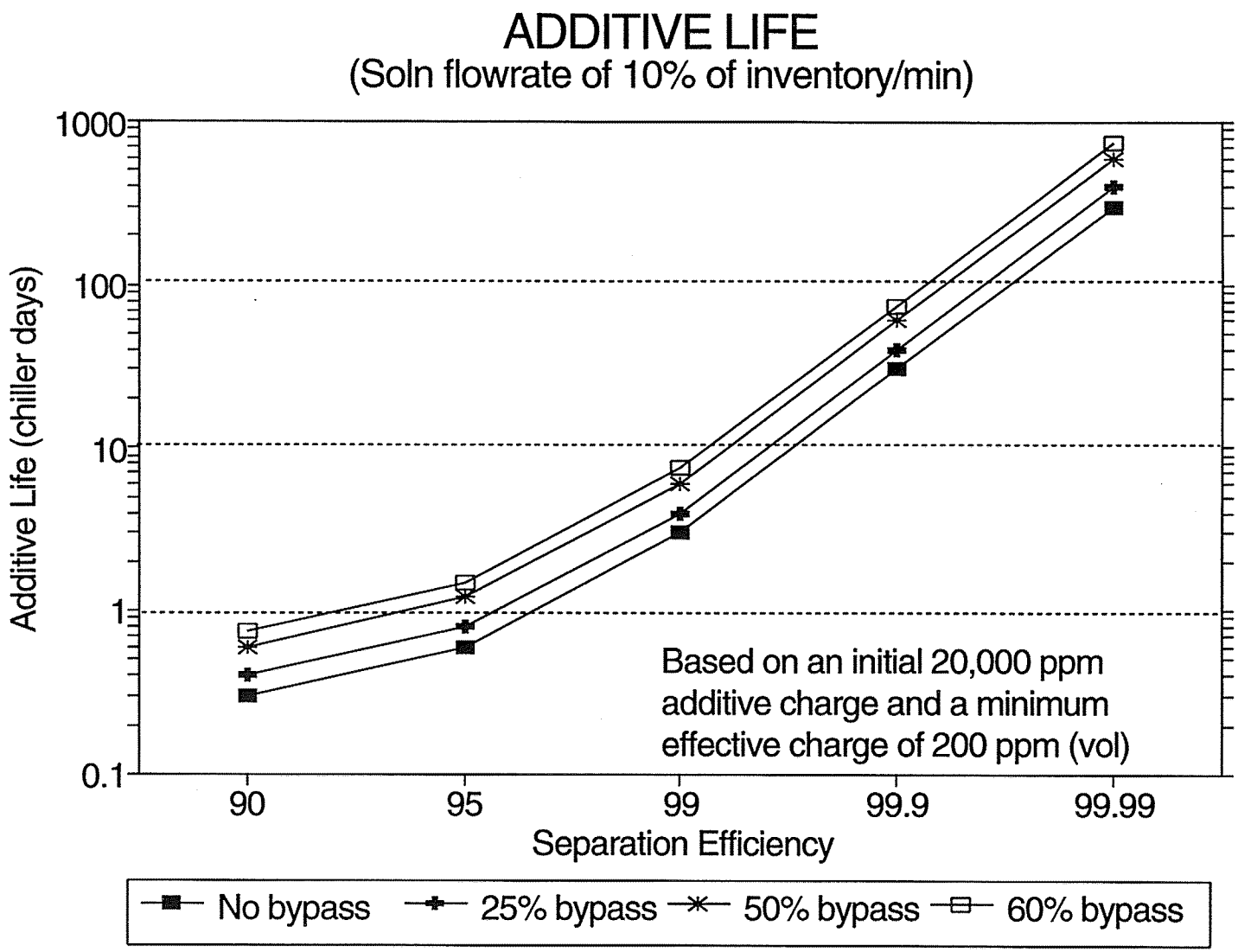

Figure 3. Summary of model predictions (10-minute residence time in separators)

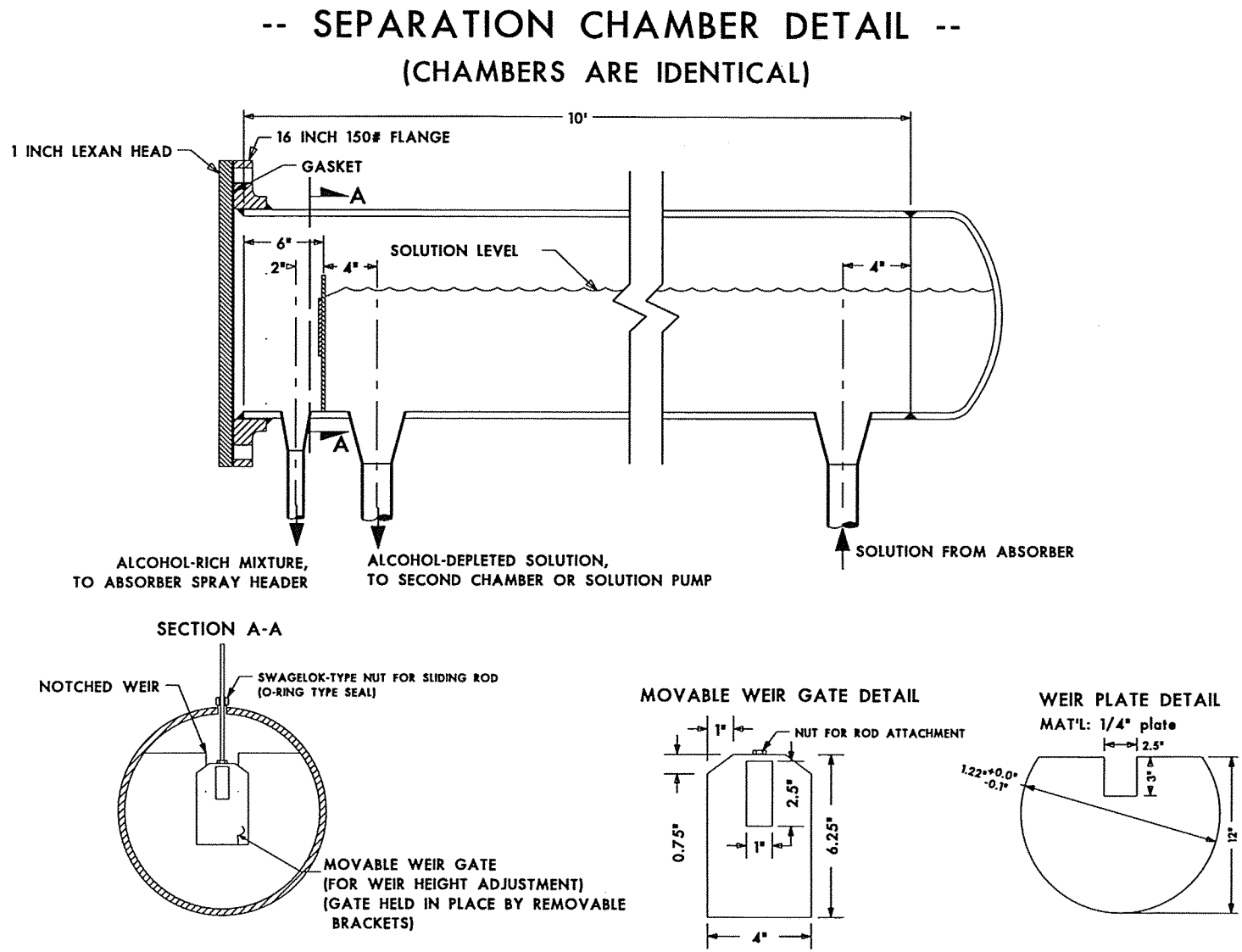

Figure 4. Detail drawing of separation chambers

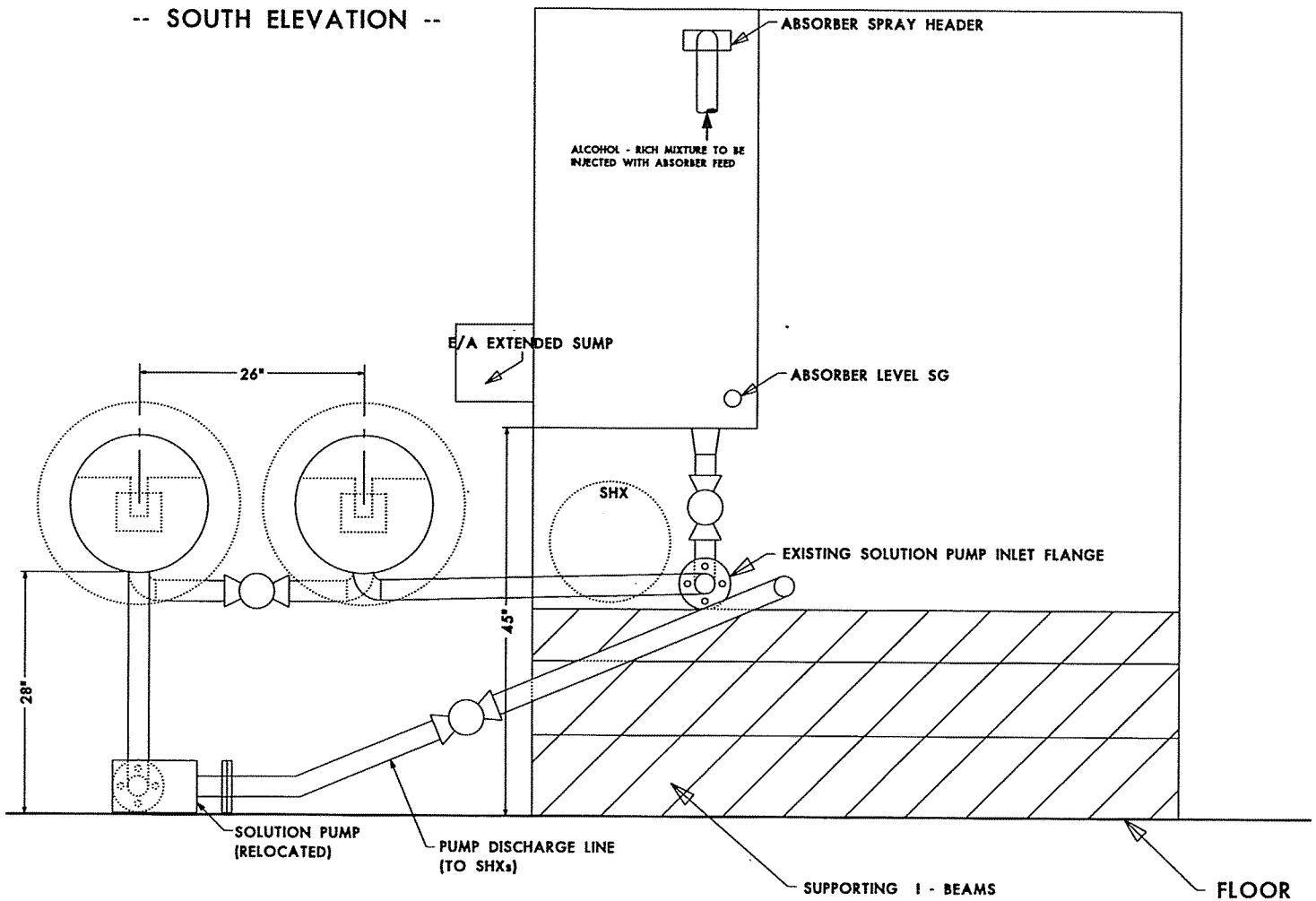

Figure 5. Elevation drawing of separation chambers, as installed

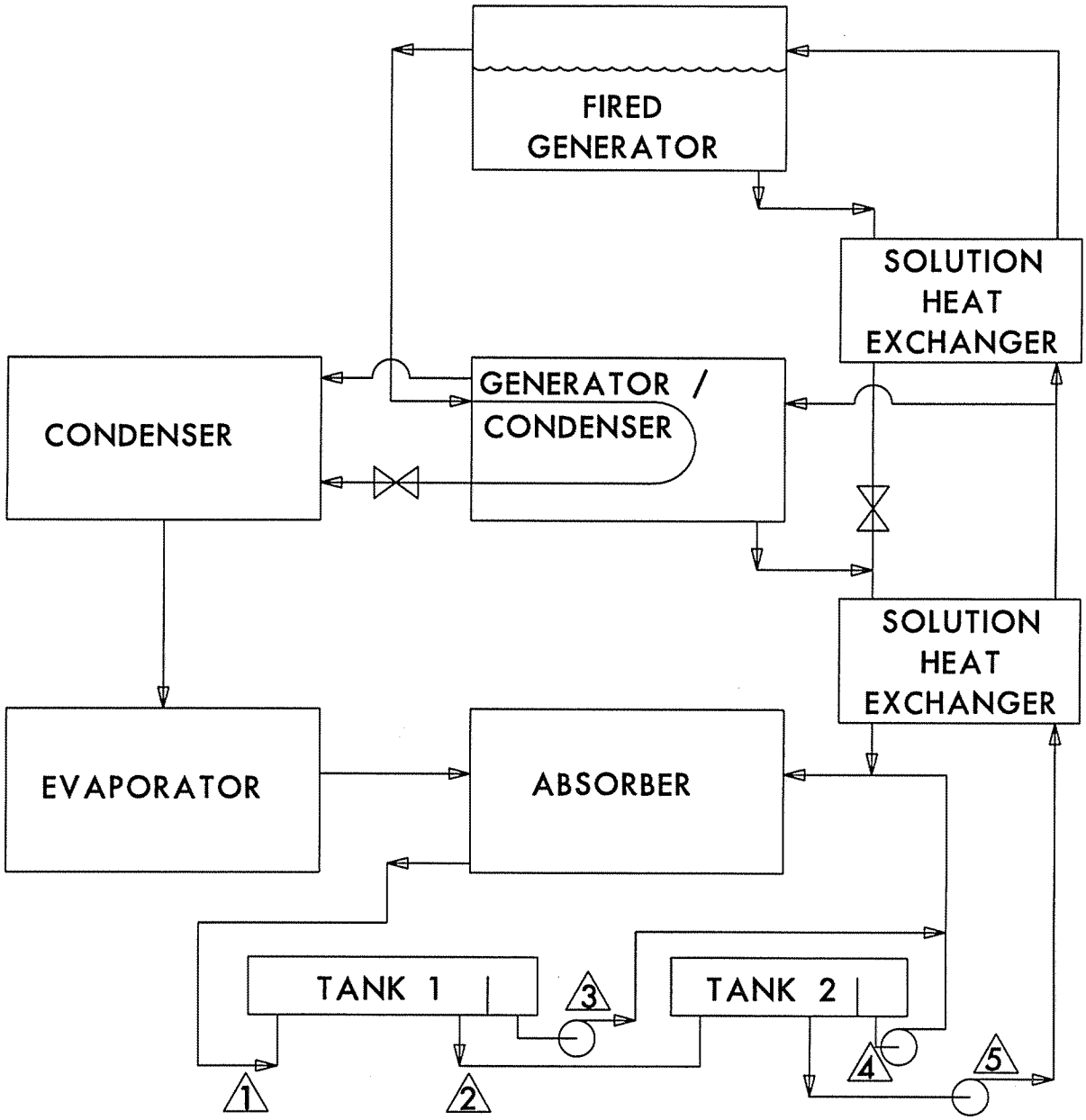

Figure 6. Schematic diagram of separation system and 40 RT chiller

Table 1. Results of Full Scale Separation Tests in a 40 RT Chiller

Sample Point	Measured Parameter	Test Number 1	2	3	4
1	2EH Conc. ppm	2230	1818	3084	973
1	Soln Flow gpm	16	16	16	16
1	2EH Flow gpm	0.0357	0.0291	0.0493	0.0156
2	2EH Conc. ppm	1430	1575	2279	702
2	Soln Flow gpm	12	15.4	12	15.4
2	Soln Flow gpm	0.0172	0.0243	0.0273	0.0108
3	2EH Conc. ppm	16397	112274	21583	20956
3	Soln Flow gpm	4	0.6	4	0.6
3	2EH Flow gpm	0.0656	0.0674	0.0863	0.0126
4	2EH Conc. ppm	3582	15428	6455	3954
4	Soln Flow gpm	4	0.6	4	0.6
4	2EH Flow gpm	0.0143	0.0093	0.0258	0.0024
5	2EH Conc. ppm	2213	1878	2461	793
5	Soln Flow gpm	8	14.8	8	14.8
5	2EH Flow gpm	0.0177	0.0278	0.0197	0.0117
Overall	Separation Efficiency	0.50	0.04	0.60	0.25

Points 5 and 1. The four tests evaluated the effect of variations in the solution flow rate to the separators and the internal solution volume in the separator chambers. Note that the separation efficiency varied from 4 percent to 60 percent, far below the efficiencies desired. The solution volume in the separators doubled the solution charge required for the entire chiller for the test giving the best results, so using more solution to increase separation time and efficiency is probably not cost-effective.

The intermediate sample points showed a disturbing result in three of the four tests. In these tests, the additive flow rate at Point 3 was higher than the additive flow rate in the solution line from the absorber (Point 1). In a steady-state test such results are not possible. These tests were thought to be steady-state tests, since the data were taken only after several hours of chiller operation and when thermal steady-state had been attained.

A subsequent test showed that, despite the attainment of thermal steady-state, i.e., only small changes in evaporator temperatures and cooling load, there were still significant transients in the additive concentration in the separation system and in the chiller. Figure 7 shows the results of one long-duration test where the additive concentration at the absorber exit was measured 21 times during an 8.5 hour period. The results shown in Figure 7 were all recorded after thermal steady-state was attained. These results show that the additive circulation was definitely not in steady-state during the previous tests, thus providing an explanation for the conflicting intermediate results of Table 1. No further testing was conducted due to the expected low separation efficiency of the gravity separation technique and the expectation that longer tests would not simulate actual chiller operation well.

The efficiency of the separation system could be increased by increasing the residence time for the solution in the separation chamber. However, for a fixed solution flow rate, increasing the residence time requires increasing the volume of solution in the chamber, thus increasing cost and making the economics even worse.

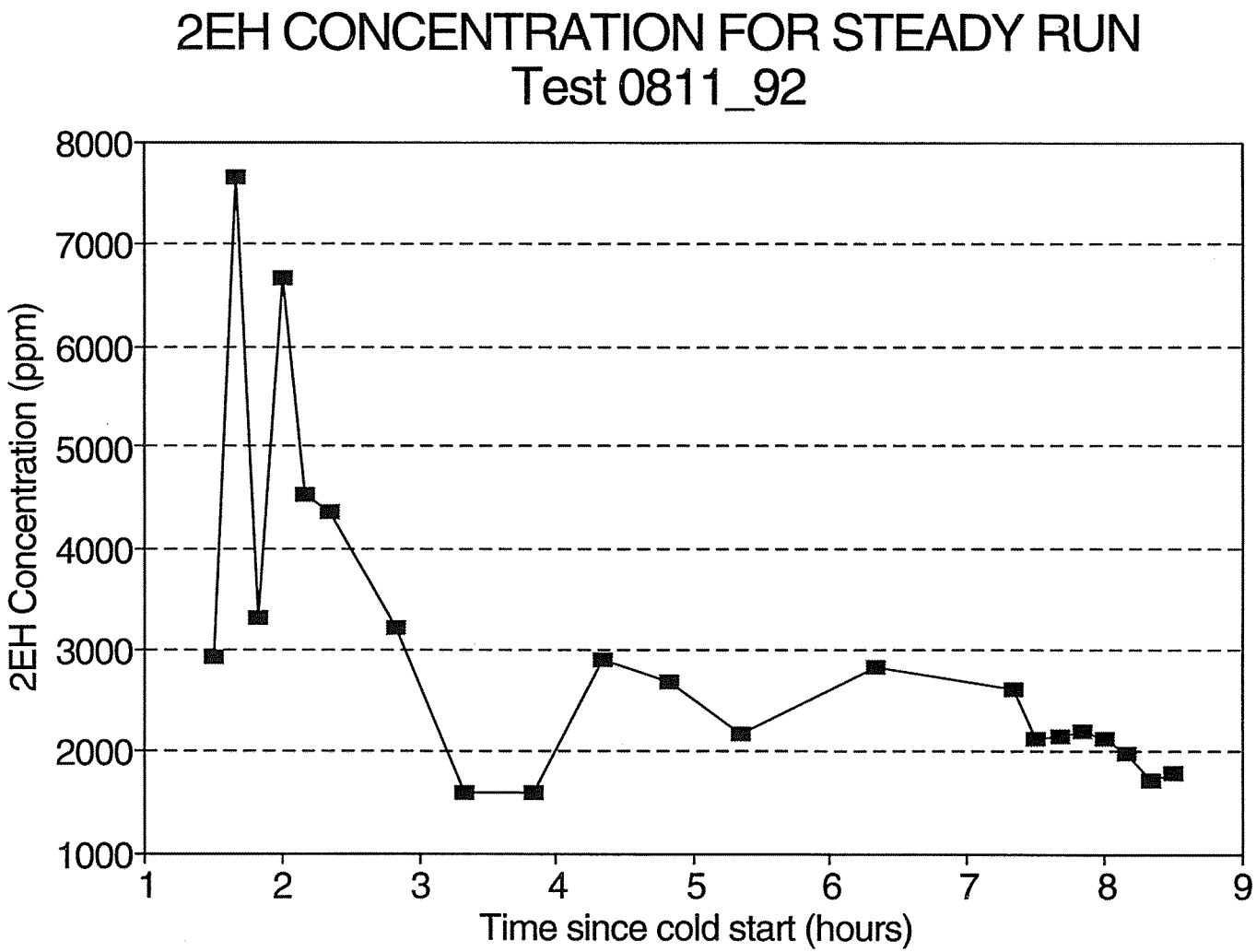

Figure 7. Additive concentration at the absorber exit during an extended test

The conclusion is that additives such as 2EH probably cannot be economically separated from the solution in gravimetric or reboiler chambers. The alternatives, then, are to only use additives with high-temperature stability, to continue to use 2EH as the absorber additive, but to replenish the 2EH charge when high-load conditions occur, or identify and develop a new separation technique.

Alternative Additive Test

To evaluate the potential performance of an alternative high-temperature additive, 1H,1H,7H-dodecafluro-1-heptanol (DFH) was tested in the 40 RT chiller. In tests at ORNL, DFH showed an absorption enhancement of 7 percent in small-scale absorber tests. More importantly, it did not break down at temperatures up to 300 C (572°F), which is the limit of the test apparatus.

The chiller test results (using the 40RT chiller at Battelle) were interpreted using a Wilson plot to determine the absorber-side heat-transfer coefficient. Tests were conducted over a range of water-side flow rates for the test absorber, while the absorber-side conditions and the cooling water temperature were held constant. The results in Figure 8 show the overall heat-transfer resistance (1/U) as a function of the inverse of the water velocity inside the absorber tubes. Extrapolating these results to zero velocity gives a value for the inverse of the absorber-side coefficient, as shown in the following table:

Additive	Absorber-Side Heat-Transfer Coefficient
None	177 Btu/(hr-ft^2-F)
DFH	213 Btu/(hr-ft^2-F)
2EH	264 Btu/(hr-ft^2-F)

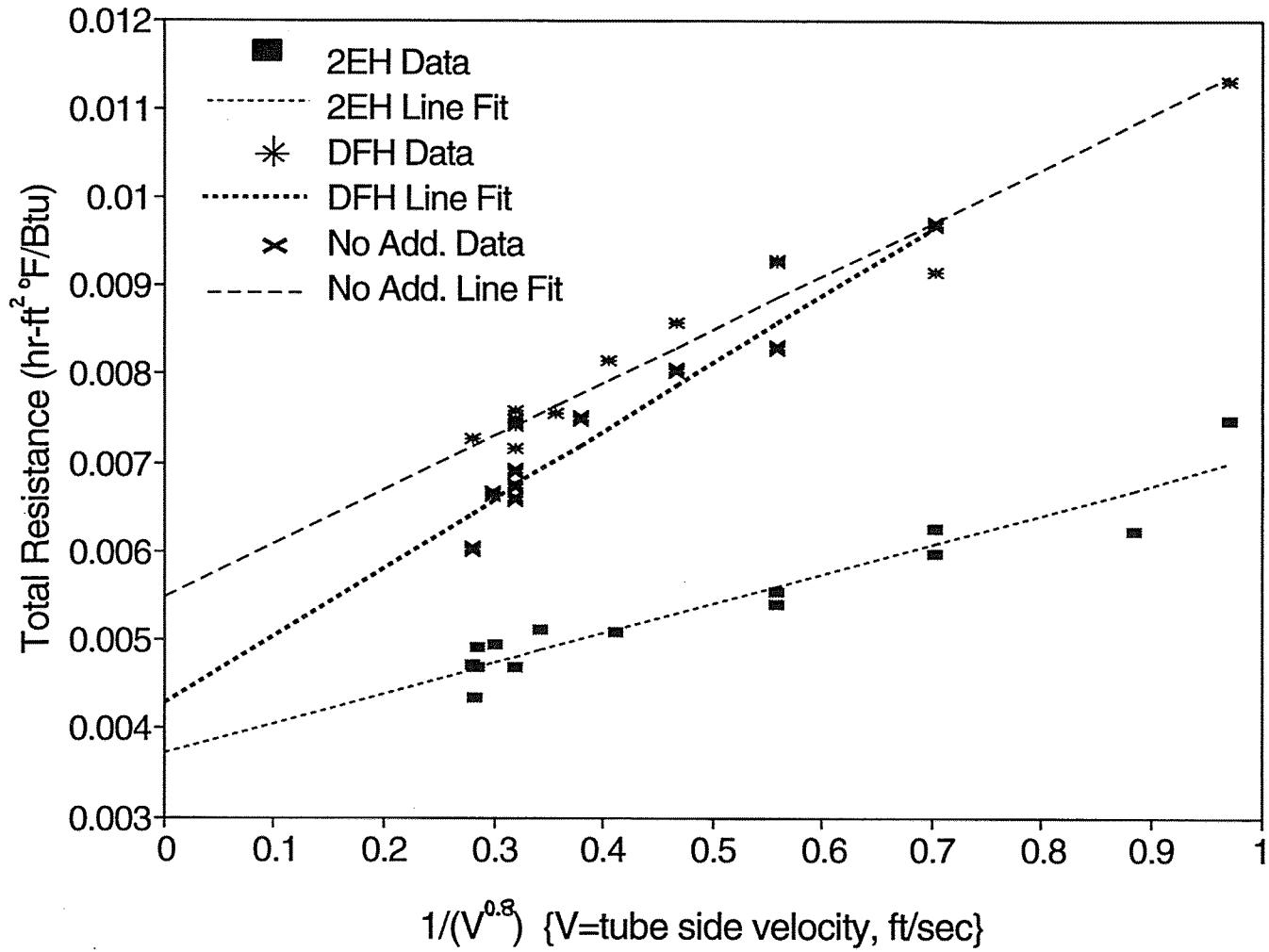

Figure 8. Wilson plot for additive tests in a 40 RT chiller

The DFH test results from the chiller showed that DFH can make a significant improvement in absorber performance. However, this performance improvement is significantly less than can be obtained with 2EH. Also, there are potentially significant chiller redesign and cost issues to be resolved before DFH can be considered a practical additive. The impact on chiller design is due to the high density of DFH. DFH is more dense than LiBr solution, even at absorber inlet conditions, so the DFH tends to sink to the bottom of any solution or refrigerant reservoir. Because present chillers are designed to allow 2EH to float on top of solution and refrigerant pools, a major change in the approach to additive management is required. Further, present designs rely on the accumulation of several gallons of 2EH on top of the condensate sump to effectively return 2EH to the absorber. This is cost-effective with 2EH (at $5 per lb), but it will not be cost-effective for DFH, which costs about $500 per lb.

Materials Compatibility Evaluations

Background

A major issue in the development of any new, higher efficiency, higher temperature absorption cycle has always been the identification of corrosion inhibitors and construction materials that are adequate for the expected operating conditions. The utilization of triple-effect cycles, such as the DCC cycle, requires peak operating temperatures of about 450°F at the generator solution exit. Thus, temperatures in the generator and solution heat exchanger will be in the 400 to 500°F range, when normal temperature variations are considered. Since current chillers usually operate at a peak temperature of 330 to 350°F, little is known about the materials compatibility issue for the higher temperature range.

The materials development effort for two residential absorption systems that used LiBr solution at up to 400°F gave some guidance in materials and inhibitor selection for testing. However, the lower temperature of these systems, 400°F maximum compared to the

400 to 500°F range, did not identify any materials/inhibitor combinations that are known to be adequate for a high-temperature chiller.

The approach defined for the materials effort on this project was to

1. Conduct a screening effort using electrochemical techniques to identify promising material/inhibitor combinations for further evaluation.

2. Conduct weight-loss coupon tests to evaluate the promising candidate combinations by measuring longer-term corrosion rates.

3. Conduct closed-loop corrosion tests with the best candidate material/inhibitor combinations where they were exposed to hot, flowing LiBr solution and the boiling action of a generator.

The objective of these efforts was to identify a set of cost-effective materials and inhibitors that could withstand the expected conditions in a triple-effect chiller, without resorting to an inhibitor, such as a chromate, that is not environmentally acceptable upon disposal. The initial expectation was that only one inhibitor compound might prove to be useful following the weight-loss coupon tests. However, these tests showed the potential for a second, new inhibitor, leading to a second series of weight-loss coupon tests in the project.

Electrochemical Coupon Testing

The initial plans and efforts were directed toward finding one good material/ inhibitor combination for comparison with the same material and a chromate-based inhibitor. The screening tests involved electrochemical coupon tests to evaluate a number of materials and three potential inhibitors for use at temperatures up to 450°F. Chromate was included in the test series as the baseline because of its widespread use as an inhibitor in LiBr chillers. Molybdate was chosen as the second inhibitor because of its promise of good inhibition at up

to 400°F, its use in lower temperature chillers and its environmental acceptability. There was no clearly good choice for the third inhibitor as this project was initiated.

Early in the project, silicate was identified as a potential inhibitor, but little was known about its performance. Since the topic of corrosion inhibition in LiBr solutions has received so much attention in the development of LiBr absorption technology, there were no high expectations for being able to find a new, improved inhibitor. Thus, the initial project plans were to take the best material/inhibitor combination from the screening tests into the comparison tests with the chromate.

Table 2 shows the materials that were tested in the electrochemical test screening. Each of these five materials was tested with three potential inhibitors, listed in Table 3. Figure 9 shows a schematic of the electrochemical polarization test apparatus. The specimen and counter electrodes were used to impress a potential between the specimen and the solution. The potential between the specimen and the reference electrode and the corrosion current were measured as the test results. Figure 10 shows the idealized results of such a test. A good material/inhibitor combination will show low current in all ranges and a wide potential difference in the passive range.

Test results for two of the alloys tested, carbon steel (C1018) and alloy 2205, are shown in Figures 11 and 12. The carbon steel results show that the molybdate inhibitor has higher values of corrosion current than the chromate inhibitor, and a narrower passive range. However, the molybdate results are much better than those for the silicate inhibitor. Figure 12 shows that there is little overall difference between the molybdate and silicate inhibitors. Neither is as good in this test as the chromate, however. Alloys 316L and Ni200 showed low corrosion currents, but no strong basis for choosing one particular inhibitor.

Generally, the electrochemical test results indicated that a range of alloys between the carbon steel, the lowest cost alloy, and much more costly alloys such as 316L and 2205, offered significant potential for withstanding the LiBr corrosion at 450°F. The

Table 2. List of Alloys Tested in Electrochemical Tests, Their SAE Class, and Their Composition

Alloy	SAE Class
C1018	Carbon Steel (0.18C)
CDA706	Copper-Nickel (90Cu-10Ni)
316L	High Alloy Steel (18Cr-8Ni-2½Mo)
2205	High Alloy Steel (22Cr-5Ni-3Mo)
Ni200	Nickel (99½Ni)

Table 3. Inhibitor Formulations

Chromate Solution: (Li_2CrO_4)	
H_2O	To make 1 liter
LiOH	2.4 g/l
$Li_2CrO_4 \cdot 2H_2O$	1000 ppm CrO_4
LiBr	53% (870 g/l)
Molybdate Solution: ($LiMoO_4$) (Foote Mineral Co. Patent, 1965)	
H_2O	To make 1 liter
LiOH	2.4 g/l
Li_2SO_4	325 mg/l
$LiMoO_4$	700 mg/l (4 mg/cm^2 of coupon area)
LiBr	53% (870 g/l)
Potassium Silicate Solution: (K_2SiO_3)	
H_2O	To make 1 liter
LiOH	2.4 g/l
K_2SiO_3	2 ml/l
LiBr	53%

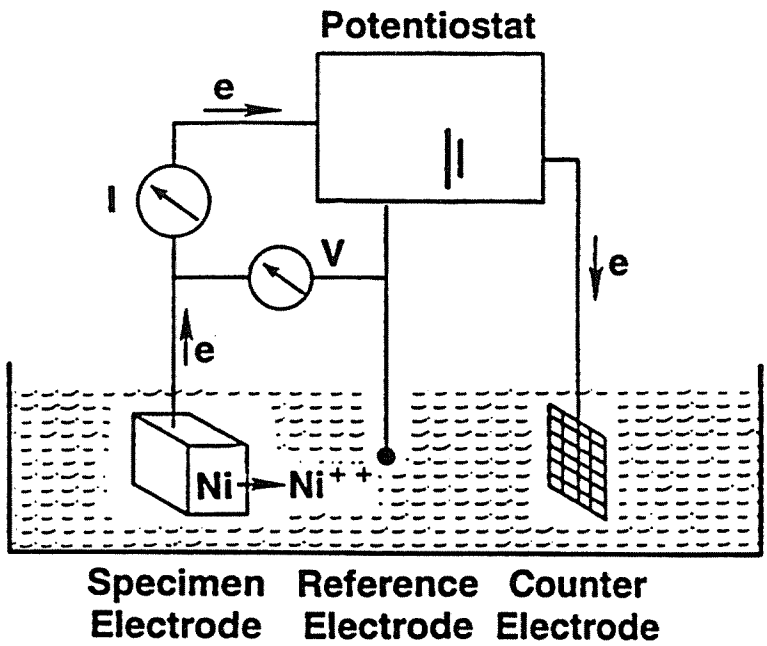

Figure 9. Electrochemical polarization test schematic

alloys recommended for testing using weight-loss coupons are given in Table 4. This table includes those alloys tested with the electrochemical technique and several additional alloys of intermediate cost and good potential for adequate corrosion resistance. The electrochemical test results showed that both new inhibitors showed potentially good results, but no clear basis for choosing one inhibitor or the other or any particular material. The choice of materials for the weight-loss coupon tests was expanded so that more practical results might be obtained.

Weight-Loss Coupon Testing

The weight-loss coupon tests were conducted using the standard procedure for such tests at Battelle. Standard coupons were weighed, paired, and placed in 100 ml Teflon® beakers. Several of these beakers were placed in a one-gallon autoclave for the test duration. The autoclave was evacuated to vacuum conditions and heated to test temperature for either

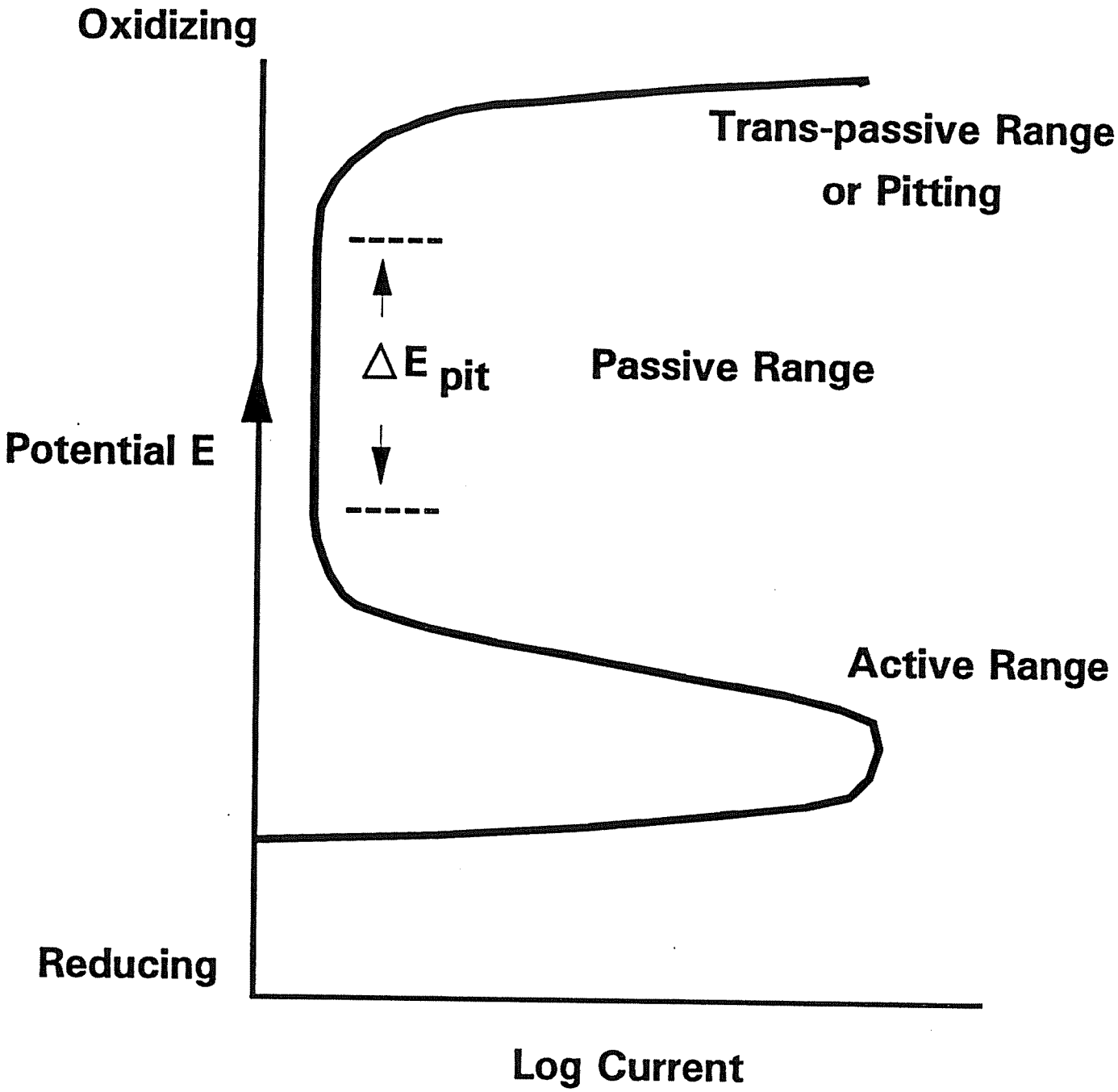

Figure 10. Idealized polarization test results

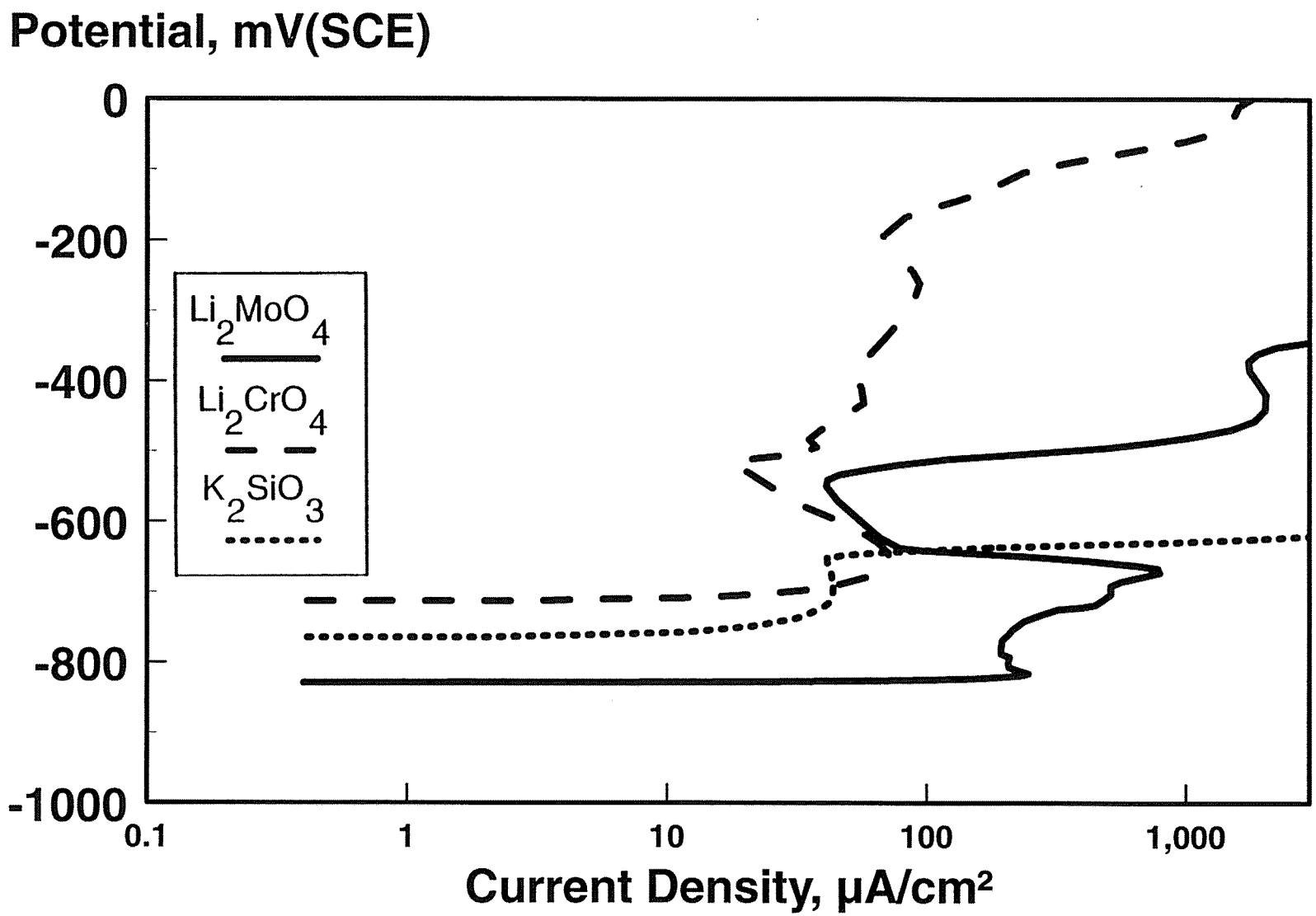

Li450F2A

Figure 11. Polarization test results for alloy C1018 at 450°F

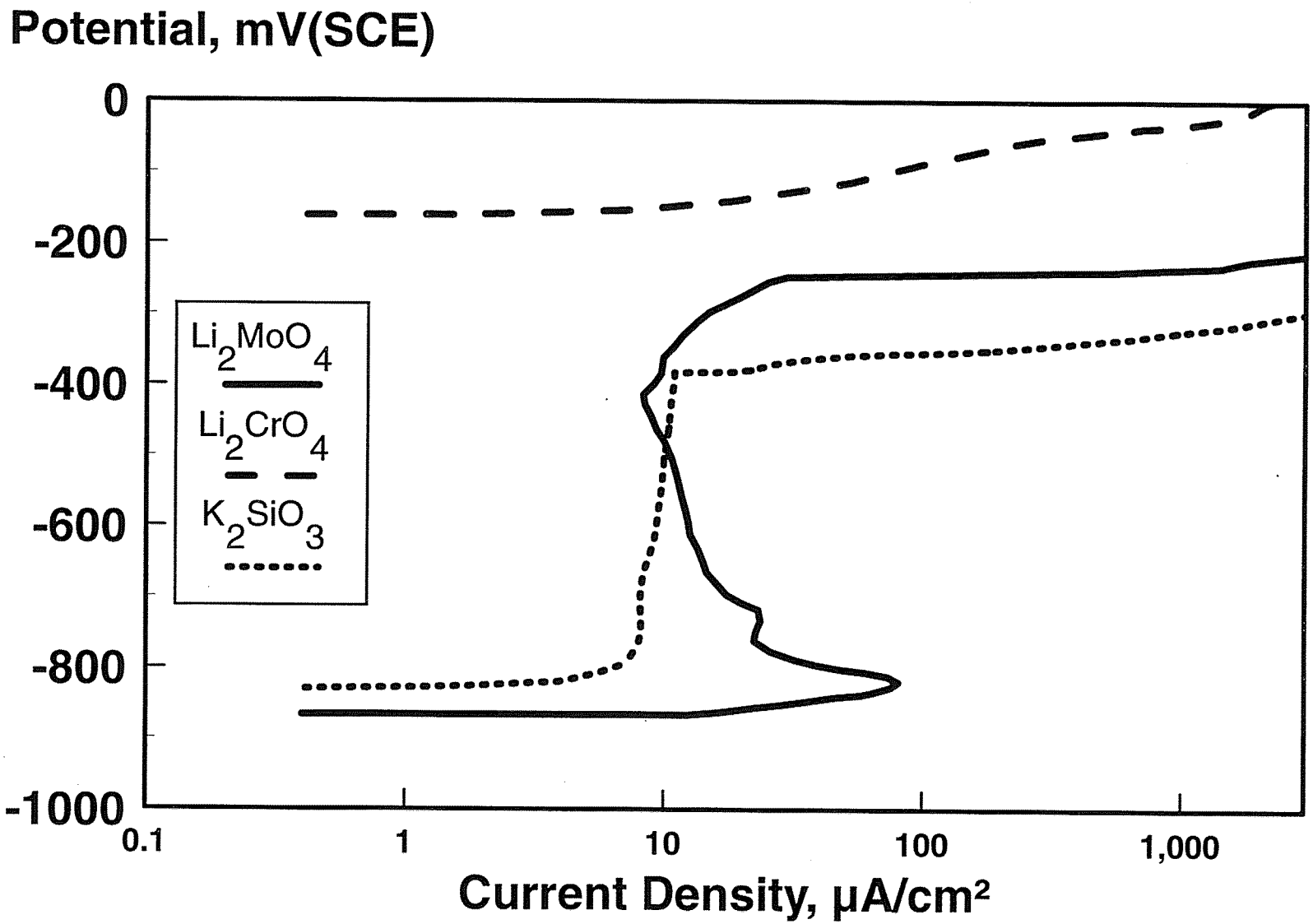

Li450F2D

Figure 12. Polarization test results for alloy 2205 at 450°F

Table 4. List of Alloys Tested in Weight-Loss Tests, Their SAE Class, and Their Composition

Alloy	SAE Class	Geometry*
C1018	Carbon Steel (0.18C)	C, TD
8620	Low-Alloy Steel (½Cr-½Ni)	C
F11	Low-Alloy Steel (1¼Cr-½Mo)	C, TD
F22	Low-Alloy Steel (2¼Cr-1Mo)	C, TD
CDA706	Copper-Nickel (90Cu-10Ni)	C, TD
316L	High Alloy Steel (18Cr-8Ni-2½Mo)	C, TD
2205	High Alloy Steel (22Cr-5Ni-3Mo)	C, TD
Ni200	Nickel (99½Ni)	C
TiGr2	Titanium (99Ti, commercial purity)	C, TD

* C = Flat Coupon, TD = Tear-Drop

32 or 64 days. When the tests were completed, the coupons were descaled, weighed and analyzed following ASTM G-1 practice. The coupons were photographed, and annualized average corrosion rates were calculated. Copies of key coupon photographs are presented in Appendix A.

Figures 13 to 15 show the results of 32- and 64-day coupon tests for several materials in each of the three inhibitors tested. These results are from tests of flat coupons, with the coupons fully immersed in the inhibited solution. These tests simulate the conditions in the liquid solution-to-solution heat exchanger of a chiller and are important because of the large surface area of material in the heat exchanger. The flat coupons are used to provide a more accurate measure of corrosion rate, and the tear-drop coupons provide a measure of corrosion rate and susceptibility to stress corrosion cracking.

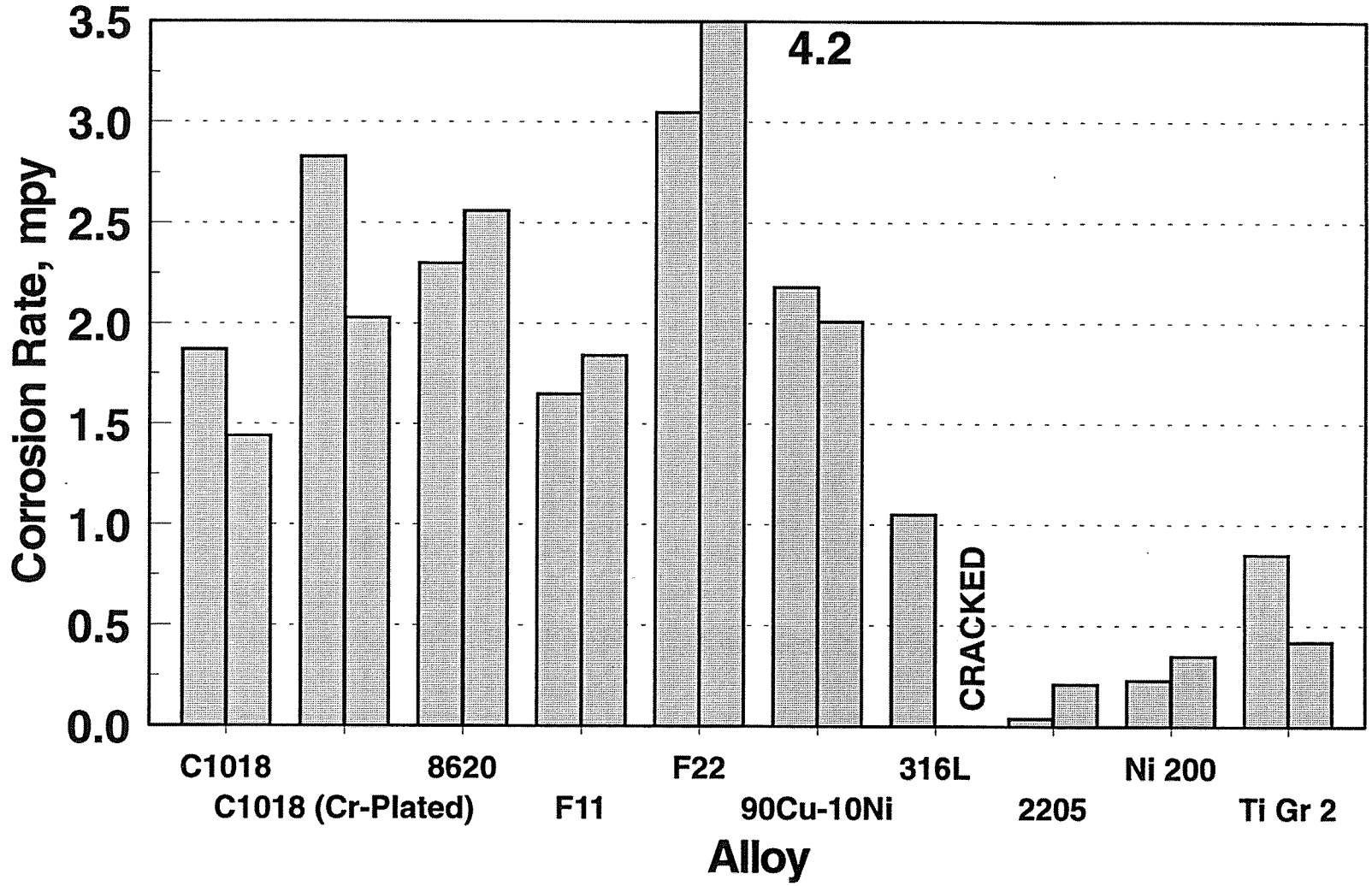

autocl-4

Figure 13. Corrosion rate results for chromate inhibitor at 450°F for 32 days, fully immersed flat coupons

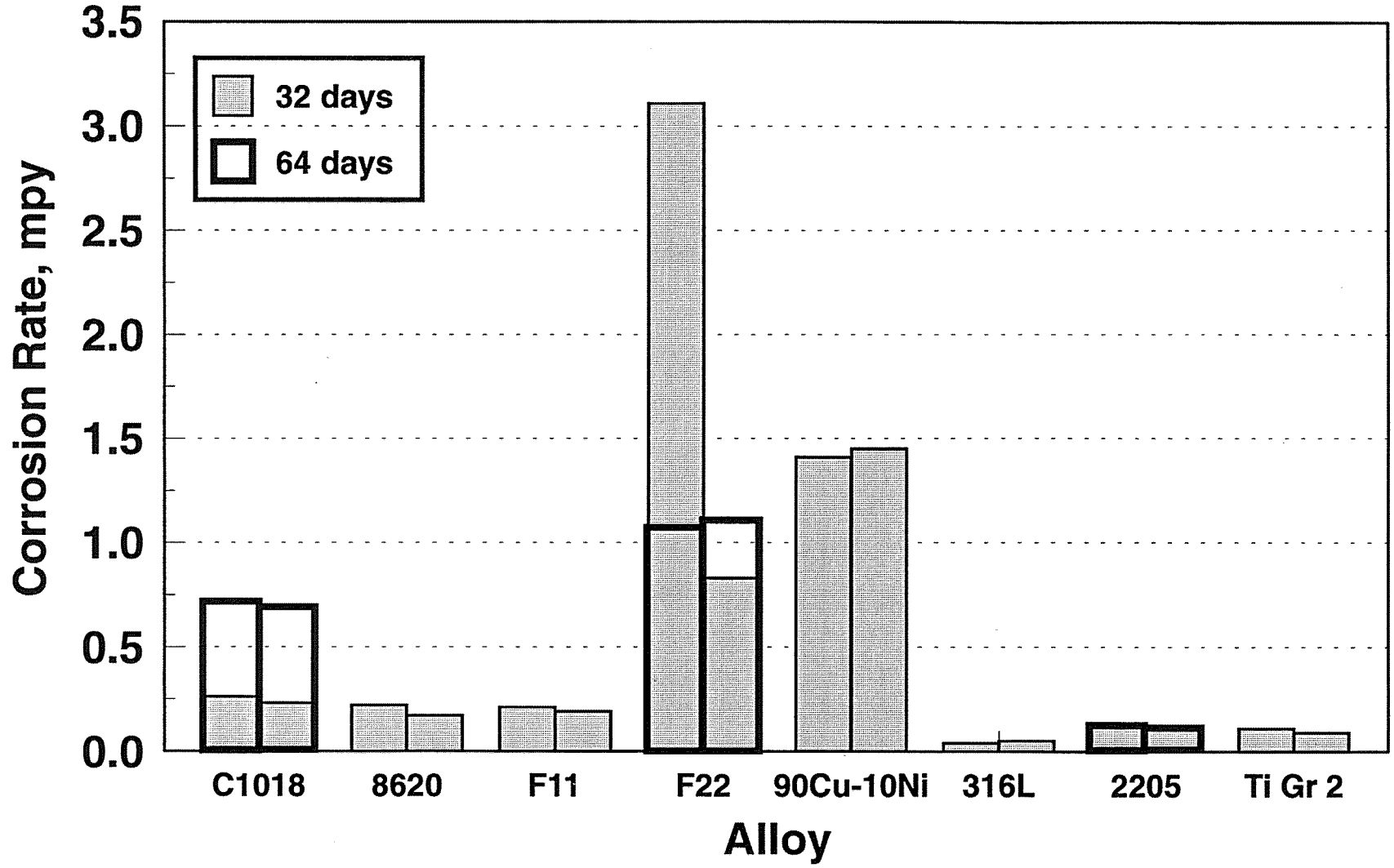

autocl-1

Figure 14. Corrosion rate results for molybdate inhibitor at 450°F for 32 and 64 days, fully immersed flat coupons

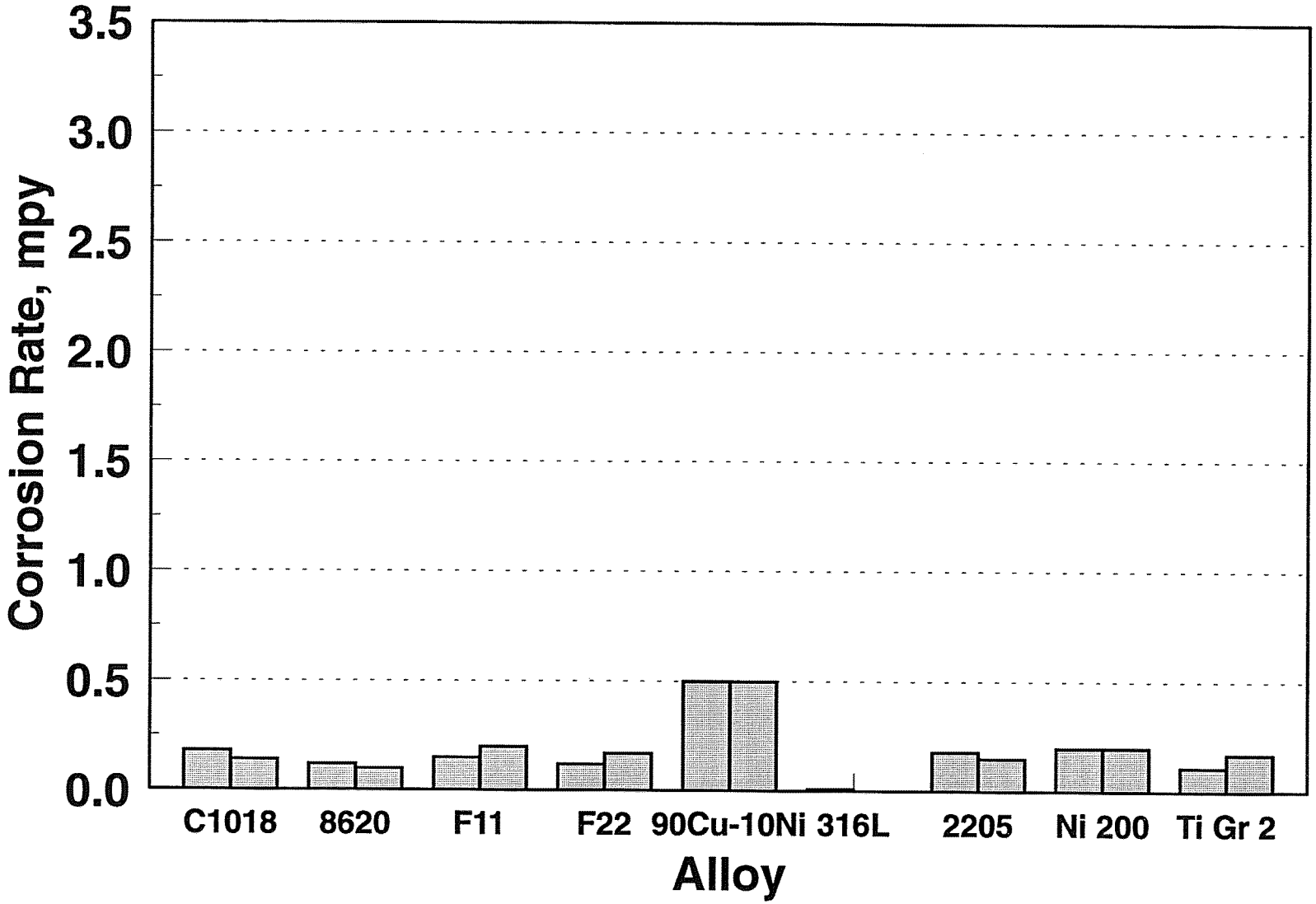

autocl-3

Figure 15. Corrosion rate results for silicate inhibitor at 450°F for 32 days, fully immersed flat coupons

Figure 13 shows the annualized corrosion rate for flat coupons fully immersed in chromate-inhibited solution at 450°F. A photograph of these coupons is presented in Figure A-1. Alloys 316L, 2205, Ni200 (pure nickel) and TiGr2 were the only ones to show a rate less than 1 mil/year (mpy). A rate of 1 mpy frequently has been considered the maximum tolerable corrosion rate in an absorption system. Thus, at 450°F there are no low-cost alloys that can perform adequately. The results for alloy 316L actually show the rate for two coupons, but one of them had a zero mpy rate, while the other was just over 1 mpy. This latter coupon also had a small stress crack (shown in Figure A-2), despite the fact that it was a flat coupon with no added stresses; the crack may have contributed to the apparently high corrosion rate. Two special chrome-plated carbon steel coupons were included in this test to evaluate an alternative to using only the chromate inhibitor.

The following table lists the materials tested in approximate order of increasing cost. Carbon steel costs are relatively stable over time, but alloying elements vary widely in cost. Hence, the materials costs and even the exact order given here are subject to change with market conditions.

Construction Materials In Order of Increasing Cost
C1018
8620
F11
F22
90Cu-10Ni
304
316
2205
TiGr2

Figure 14 shows the results of similar tests (flat coupons, fully immersed, 450°F) in molybdated solution. The photographs of these coupons are shown in Figure A-3. Only the 90Cu-10Ni alloy and alloy F22 showed corrosion rates over 1 mpy. All of the other alloys, including a plain carbon steel, showed encouraging results. There is no explanation for the comparison of the 32-day and the 64-day test results for C1018. The 64-day test was expected to show the lower of the two rates.

Figure 15 shows the results for the silicate inhibitor (flat coupons, fully immersed, 450°F): all alloys tested had a corrosion rate of less than 0.5 mpy. The photographs of these coupons are shown in Figure A-4. The accuracy of all these test measurements is considered to be plus or minus 0.5 mpy, so for most alloys the silicate is probably better than the molybdate, but little significance can be attached to this conclusion. The significant improvements were for alloys 90Cu-10Ni and C1018. These results are for coupons fully immersed in solution, so they are directly applicable to the solution-to-solution heat exchangers for which carbon steel has been the preferred material in many chillers. It appears that the silicate inhibitor allows the use of low-cost carbon steel in one of the largest heat exchangers in a high-temperature chiller.

Another series of coupon tests was conducted using flat coupons that were only partially immersed in the inhibited solution. These tests are relevant to conditions in a generator where there is a liquid/vapor interface due to the boiling action in the generator. (The coupons in this test series were subjected to the interface, not the actual boiling.) Many of the same alloys were tested. Alloy C1018 was dropped from these tests because it showed a high corrosion rate at 400°F in both molybdate and chromate, and some of the more costly alloys, such as TiGr2 and Ni200, were also dropped. The solutions were inhibited with either chromate (base case) or silicate, for which no previous experience existed.

As shown in Figures 16 and 17, neither inhibitor gave good protection to the cupro-nickel alloy. Similarly, alloy 8620 had an unacceptable corrosion rate in the chromated

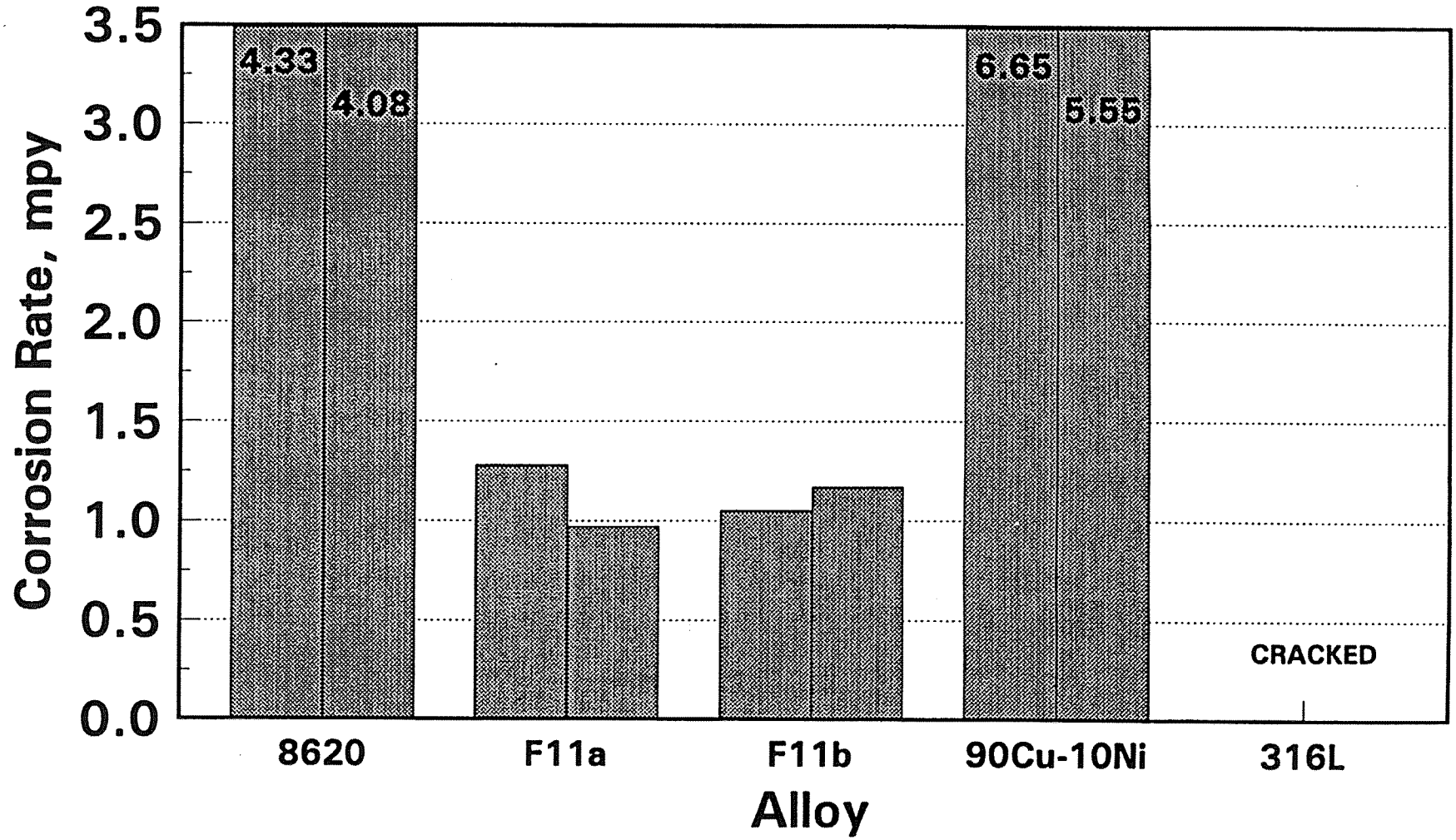

autocl-6

Figure 16. Corrosion rate results for chromate inhibitor at 450°F for 32 days — partially immersed flat coupons

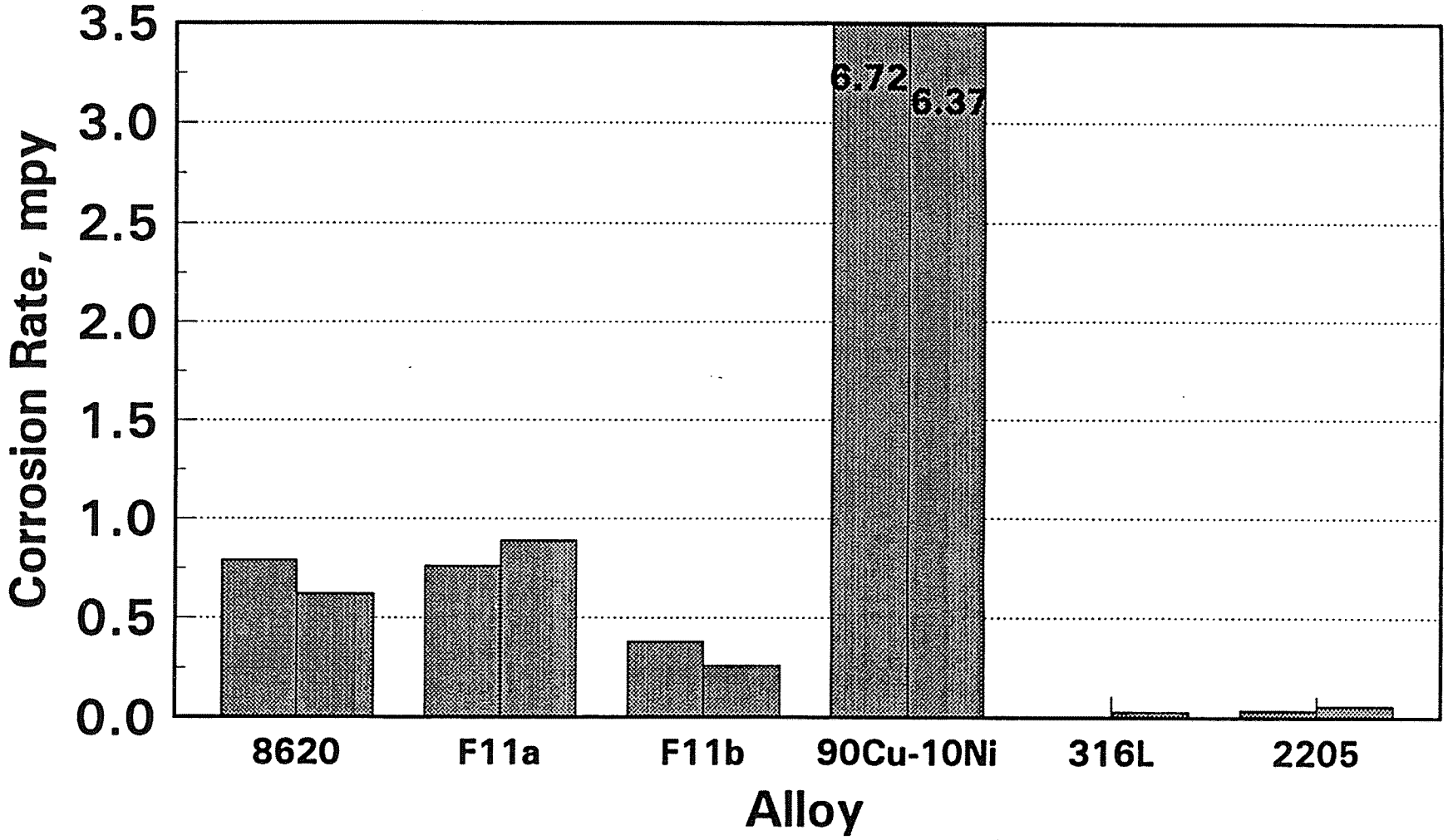

autocl-5

Figure 17. Corrosion rate results for silicate inhibitor at 450°F for 32 days — partially immersed flat coupons

solution. The remaining alloys — F11, and 316L — did well in both inhibitors, alloy 2205 also did well in the silicate inhibitor. The differences between chromate and silicate for alloy F11 are potentially significant. Fortunately, the lower corrosion rates occurred in the silicate, the environmentally acceptable inhibitor. Four F11 coupons were tested in each inhibitor, hence the labels F11a and F11b. Both 316L and 2205 gave exceptionally low corrosion rates in these tests. The photographs of these coupons are shown in Figure A-5.

An additional finding not shown on these charts, but potentially significant, is that cracks were observed in three of the four 316L coupons tested in chromated solution, while none of the four 316L coupons tested in the silicated solution cracked. All these tests were conducted in technical grade LiBr, which contains less chloride than refrigeration grade LiBr. (Chloride content of LiBr solutions was briefly evaluated in a later test series in this project.)

In summary, the partially immersed coupon tests showed that alloys F11, 316L, and 2205 exhibited acceptable corrosion resistance and have good potential when used with a silicate inhibitor. These results showed that two inhibitors, molybdate and silicate, have the potential for good corrosion inhibition of alloys 2205, 316L, F11, and C1018. The results indicate that there are additional candidates for use as an inhibitor, but little is known about these combinations beyond their promising performance in these coupon tests. A second series of weight-loss coupon tests was conducted to more completely evaluate the use of both the molybdate and silicate inhibitors.

Additional Coupon Tests

The second series of coupon tests was designed to provide additional information on the performance and possible limitations of both the molybdate and silicate inhibitors prior to building and testing corrosion loops.

Table 5 gives the matrix of conditions for these additional coupon tests. These tests focused on the following key issues:

- The performance of both the silicate and molybdate inhibitors at higher LiBr concentrations.
- The performance of both the silicate and molybdate inhibitors at higher temperatures.
- The consideration of alloys 304L and 409.
- The effect of chloride concentration on stress corrosion cracking of alloys 304L and 316L with partially immersed coupons.
- The effect of different levels of hydroxide concentration in the inhibitor, especially in the silicate-inhibited solutions.

In previous tests on this project (and many of our other previous tests), solutions having an initial concentration of 53 percent LiBr by weight were used. During the course of the tests, some water always was vaporized from the solution samples, so the final concentrations were always slightly higher than 53 percent. Nevertheless, these LiBr concentrations were not representative of the worst case situations in a chiller. These new tests were conducted at an initial concentration in the range of 60 to 62 percent. The final concentrations during the tests should be in the expected operating range for a high-temperature chiller and should still be less than 65 percent, the maximum working concentration planned for such a chiller.

Previous tests were carried out at a solution temperature of 450°F, representing an average maximum temperature for both the solution and the metal in the generator. In practice, the metal is always at a higher temperature than the solution. This is an effect that cannot be evaluated in a coupon test. However, these coupon tests were conducted at higher temperatures to give insight into the general effect of higher temperatures. These tests also will help assess the effects of generator over-temperatures which may result from a number

Table 5. Coupon Test Matrix for Addition Weight-Loss Tests

Inhibitor	Silicate					Molybdate			
Autoclave Number	1a	1b	2	3	4	5a	5b	6	7
Temperature	450 F	450 F	475 F	500 F	500 F	450 F	450 F	475 F	500 F
Additives	—	—	—	—	—	with sulfate	without sulfate	without sulfate	without sulfate
Alloy									
C1018	2 F	2 F-L 2 F-H	4 F	2 F		2 F	2 F	4 F	2 F
C1018 + Coating*			2 F	2 F			2 F	2 F	2 F
F11	2 F	2 F-L 2 F-H	4 F	2 F 2 T		2 F	2 F	4 F	2 F 2 T
409	2 F	2 F-L 2 F-H	2 F 2 T	2 F		2 F	2 F	2 F 2 T	2 F
304L	2 F	2 F-L 2 F-H	4 F 2 T	2 F	12 T**	2 F 2 T	2 F 2 T	4 F 2 T	2 F
316L			2 F 2 T	2 F	12 T**	2 F		4 F	2 F 2 T
2205				2 F 2 T				2 F	2 F 2 T
Titanium				2 F 2 T					2 F 2 T

Key: F = Flat coupon for corrosion rate measurement
T = teardrop coupon for stress corrosion cracking assessment

Notes:
1. F-L and F-H are flat coupons in low (L) or high (H) levels of LiOH.
2. All solutions are 60+ percent LiBr in water and include inhibitor.
3. Standard solutions contain approximately 300 ppm of chloride and include LiOH per Carrier or Foote Mineral Co. specifications.
4. 30 vapor space coupons are not shown.

* Nicrobraze 125 coating, approximately 0.004-inch thick
** 4T each at 30 ppm and 300 ppm chloride, 2T each at ~5 ppm and 1,000 ppm

of practical considerations. Hence, the plan was to conduct coupon tests at both 475°F and 500°F.

The promising results that were obtained previously with alloy 316L in the silicate-inhibited solution suggested the consideration of additional, lower-cost alloys in the 300 and 400 series of stainless steels. Thus, alloys 304L and 409 were evaluated in these tests.

One of the major purposes of these coupon tests was to evaluate how well the silicate inhibitor suppresses the stress corrosion cracking that is common in alloys 304L and 316L, especially in chromate-inhibited solutions. Thus, immersion coupon tests were conducted in LiBr solutions with four different chloride concentrations: 5 to 10 ppm, 30 ppm, 300 ppm, and 1,000 ppm (by weight) for this evaluation. The 5 to 10 ppm level is the lowest chloride-content LiBr solution available. The 1,000 ppm level corresponds to the standard specification for "refrigeration grade" LiBr solution. The 300 ppm level corresponds to the chloride content actually found in most "refrigeration grade" LiBr solutions. The 30 ppm level was chosen to represent a significant improvement in the chloride content of the most common solution.

It is recognized that the costs for LiBr with a low chloride content are very high. Direct extrapolation of small-quantity costs of high-purity LiBr to manufacturer costs for LiBr is not an especially accurate process, and preliminary cost comparisons are not encouraging. For example, 30-gallon drums of solution cost the equivalent of about $6/lbfor dry LiBr having 300 ppm of chloride. The small-quantity (2 to 4 lb) prices for dry LiBr are $32/lb at 99 percent purity (about 1,000 ppm of chloride) and $1200/lb at 99.999 percent purity (about 10 ppm chloride). Using the ratio of these two small-quantity prices (1200/32 = 37) gives an approximate cost of $44,000 for a 30-gallon drum of 53 percent solution, 10 ppm level. This is not meant to be a cost estimating exercise, but rather a comment that technical success (i.e., being able to use 304 in low-chloride solutions) may lead to a

requirement for considerable cost reduction efforts for the solution itself before any of the potential advantages of using alloy 304 can be realized.

It was also recognized that the hydroxide concentration is an important factor in controlling corrosion in LiBr solutions, so an initial effort was made to address that issue with the silicate inhibitor. In previous tests with the silicate inhibitor, the hydroxide concentration in the solution was that used in all the molybdate-inhibited solutions, which is widely used with other inhibitors in LiBr solutions. These tests gave generally good results, but the optimum hydroxide concentration for the silicate inhibitor is not known. Hence, the test matrix included specific tests to assess the effect of the hydroxide concentration on a few key materials in silicate-inhibited solutions. The hydroxide concentration used in the molybdate inhibitor formulation is taken from patents by Stubblefield* and Foote Mineral.**

A test matrix was developed to give variations of only one independent variable between comparable tests, making use of the results of the previous tests conducted on this project. Thus, the independent effects of increasing temperature, LiBr concentration, chloride content, and hydroxide content should be determined, despite the apparently sparse test matrix. The alloy list and alloy compositions are given in Table 6.

Results of the Additional Coupon Tests

The results of these additional weight-loss coupon tests are summarized in the following seven figures. These figures show the annualized average corrosion rates for each coupon and provide notes on particular test conditions. Figure 18 shows the effect of

---

* U.S. Patent No. 2,755,170, "Corrosion Inhibitor," Stubblefield, Edward M., Cropper, Walter V., July 17, 1956.

**U.S. Patent No. 3,218,259, "Stabilization of Lithium Molybdate Solution," Verdieck, Ralph G., Reader, Lawrence J., November 16, 1965, Assigned to Foote Mineral Corporation.

Table 6. Alloy List for Additional Weight-Loss Tests

Alloy	SAE Class (Nominal Composition)
C1018	Carbon Steel (0.18C)
C1018 + NicroBraz Coating	Carbon Steel (0.18C) + (70Ni-14Cr-5Fe-5Si)
F11	Low Alloy Steel (1.25Cr-0.5Mo)
409	High Alloy Steel (11Cr)
304L	High Alloy Steel (18Cr-8Ni)
316L	High Alloy Steel (16Cr-10Ni-2.5Mo)
2205	High Alloy Steel (22Cr-5Ni-3Mo)
TiGr2	Titanium (99Ti, Commercial purity)

varying the hydroxide concentration on the corrosion rate for four materials. Clearly, for the carbon and low-alloy steels, the hydroxide concentration is critical. It is interesting to note that the nominal concentration, taken from the molybdate practice, gave the best results of the three concentrations tested. Figures 19 and 20 show the effects of higher temperatures (475 and 500°F) on these materials. The lower alloy materials were, of course, the most susceptible to higher corrosion rates. C1018, F11, and 409 showed unacceptable corrosion rates at both 475 and 500°F. The Ni-coated C1018 samples did well at 475°F, but were marginal at 500°F, according to these results. However, the Ni coating was only 4 mills in thickness, so, even at 475°F, the coating was endangered. Once the coating was breached in one location, the resulting corrosion of the base steel proceeded rapidly. Hence, the coatings were not especially attractive or useful in this case.

Figure 21 shows the effectiveness of the silicate inhibitor as a means of preventing the onset of stress-corrosion cracking. None of the 24 samples exposed to 500°F LiBr solution cracked in the presence of the silicate inhibitor. These results are not

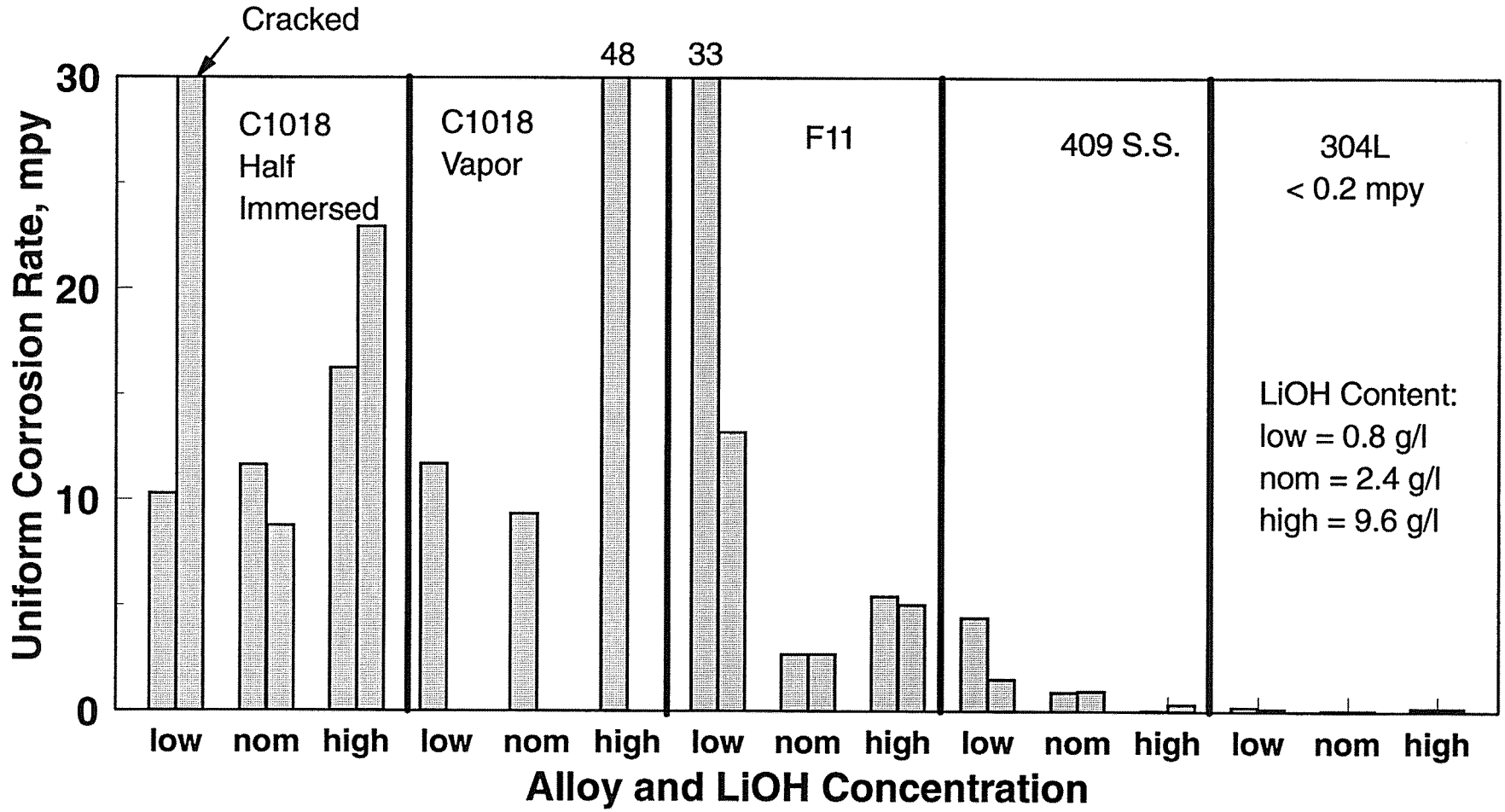

450silun

Figure 18. Corrosion rate results for three hydroxide concentrations in silicate-inhibited solutions at 450°F, fully immersed flat coupons, except as noted

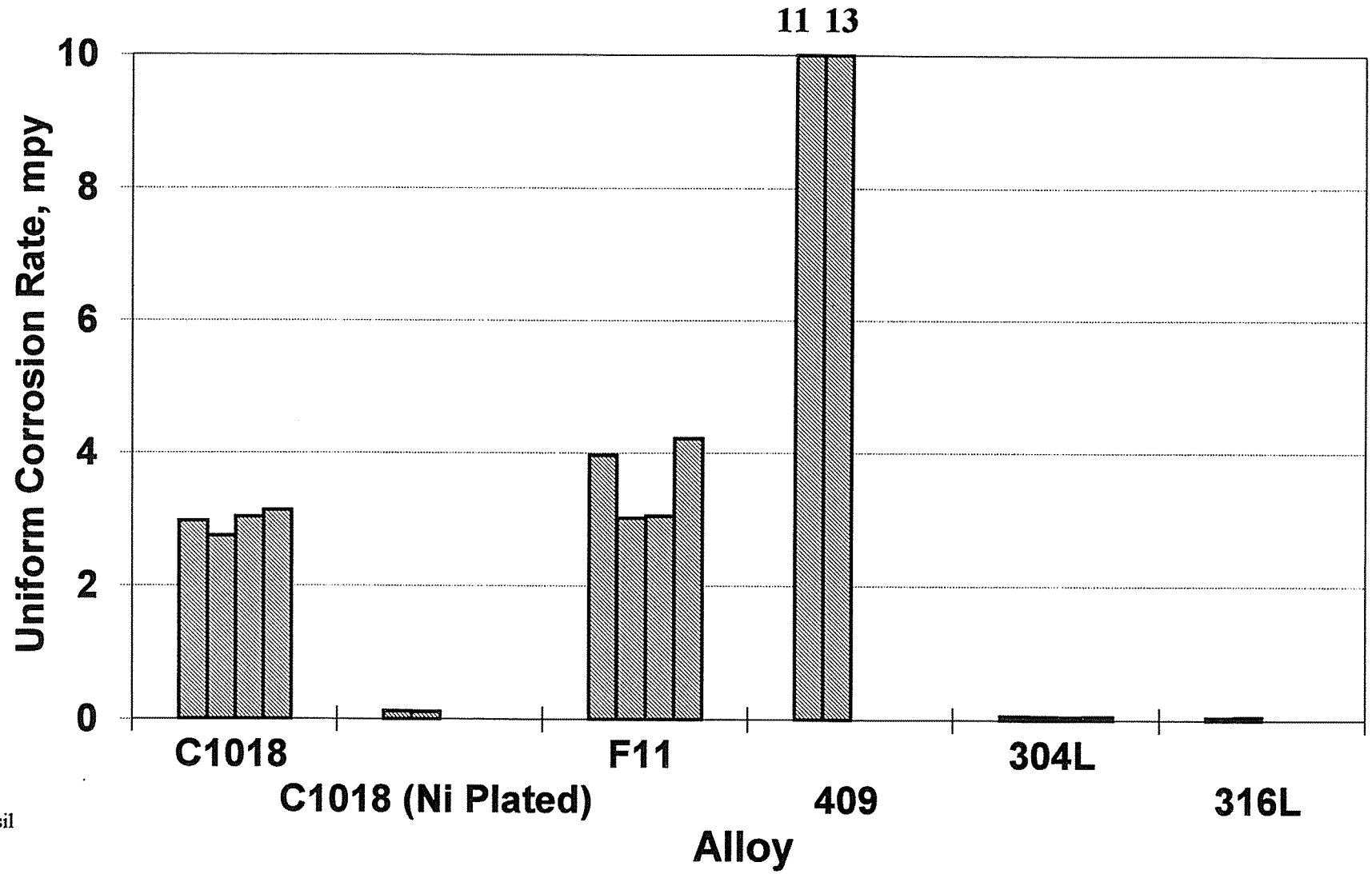

475_sil

Figure 19. Corrosion rate results in silicate inhibited solutions at 450°F, fully immersed flat coupons

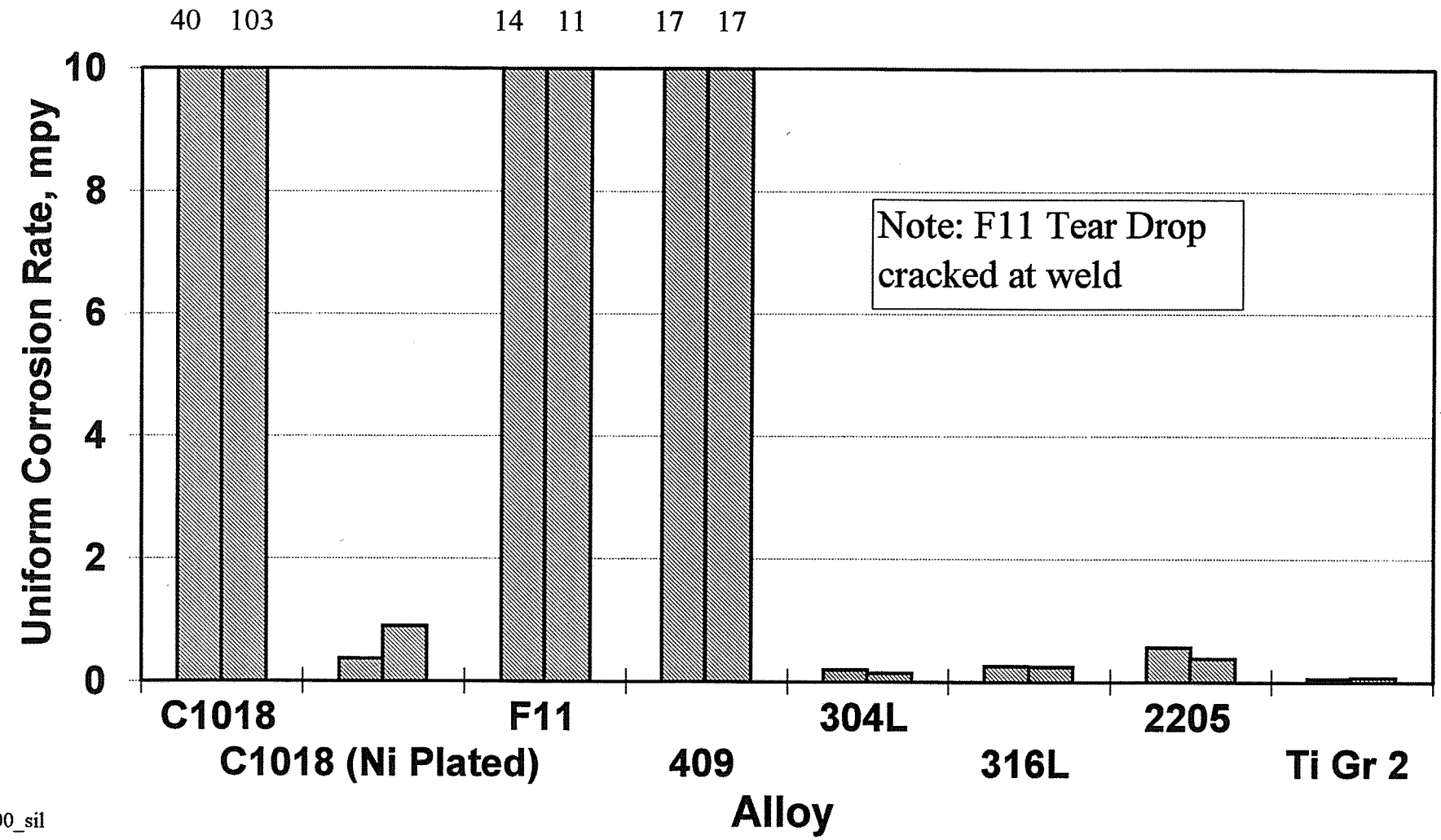

500_sil

Figure 20. Corrosion rate results in silicate-inhibited solutions at 500°F, fully immersed flat coupons

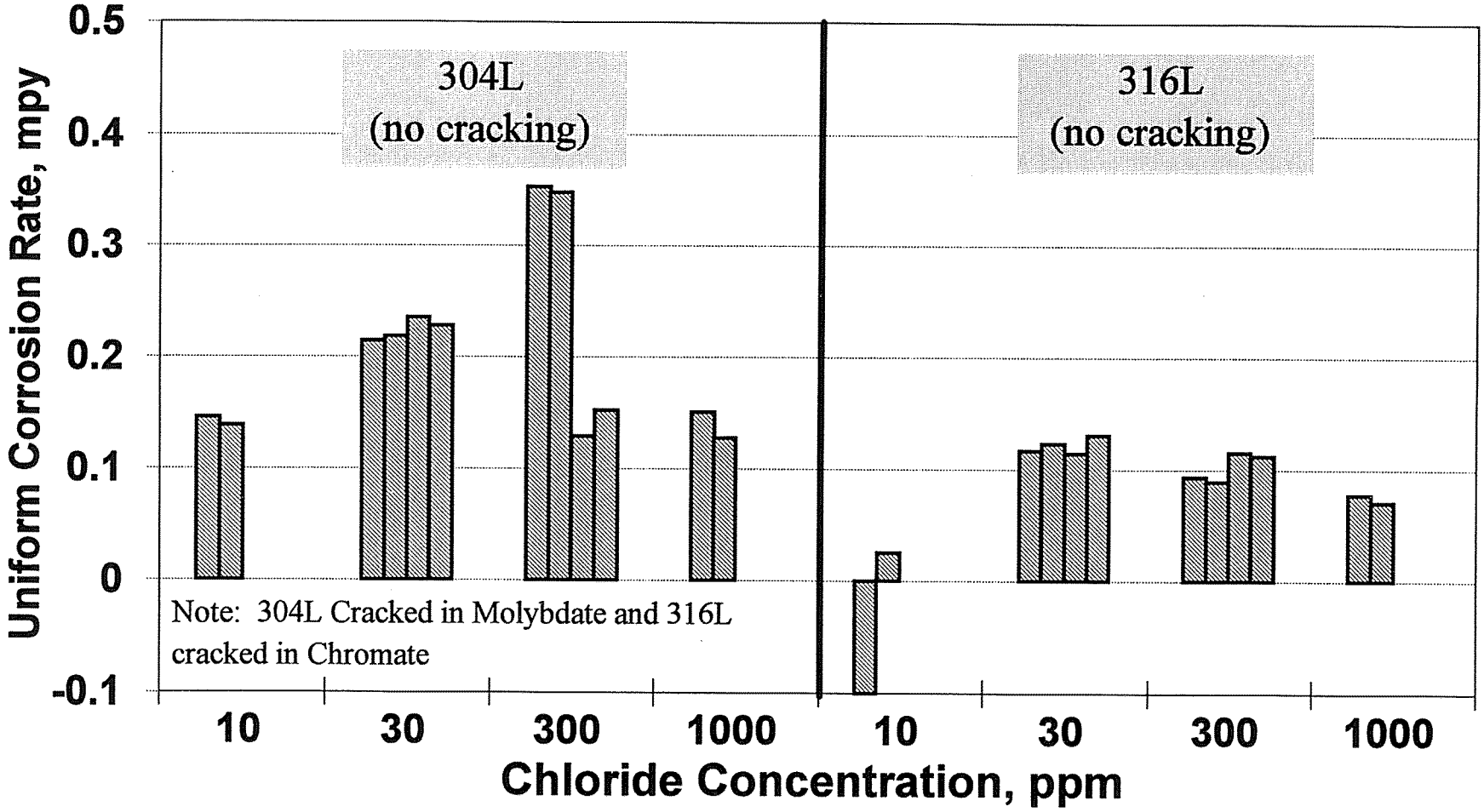

Autoclav.wb1:500_sil_cl

Figure 21. Corrosion rate results in silicate inhibited solutions at 500°F with four chloride concentrations, teardrop coupons, partially immersed

conclusive, in that they do not prove that a 300-series stainless will never crack in a silicate-inhibited solution. However, these results are in marked contrast to the experience with other inhibitors, which indicates that most 300 series stainless steel coupons will crack in less than 30 days at temperatures of 400°F and below.

Figure 22 shows the effect on the corrosion rate of using a sulfate to stabilize the concentration of molybdate in solution. The Foote mineral patent shows the use of sulfate to control the concentration of molybdate in LiBr solutions. Although the teaching of this patent is apparently not practiced in industry, the effect of the sulfate on corrosion rates was of interest. These tests showed that the presence of sulfate had no effect on corrosion rate in a test where the molybdate can only precipitate to the bottom of the test vessel. Hence, the molybdate was available to reenter the solution if solution equilibrium conditions allowed it to redissolve. Although the sulfate did not reduce the corrosion rates in this test, its presence did not increase the corrosion rate for any of the materials tested.

Figures 23 and 24 show the effects of higher temperatures (475 and 500°F) on materials of interest with the molybdate inhibitor. At these temperatures, alloys C1018, F11, and 409 showed very high corrosion rates. The Ni coating on the C1018 coupons appeared to be effective at 475°F but not at 500°F. The probable explanation of these results is that the coating was breached during the 500°F test, but had not yet been breached during the 475°F test. Extension of the 475°F test for a short additional time probably would have resulted in breaching the coating and a high corrosion rate. Only the more costly alloys — 304, 316, and 2205 — showed good corrosion resistance in these tests.

Corrosion Loop Tests

The coupon test results were reviewed with ORNL and the engineering staff at York during the process of selecting the alloys and inhibitors for the closed-loop corrosion tests. Four loops were to be built, focusing primarily on materials and inhibitors for use in a cost-effective high-temperature chiller. The test matrix for the materials and corrosion

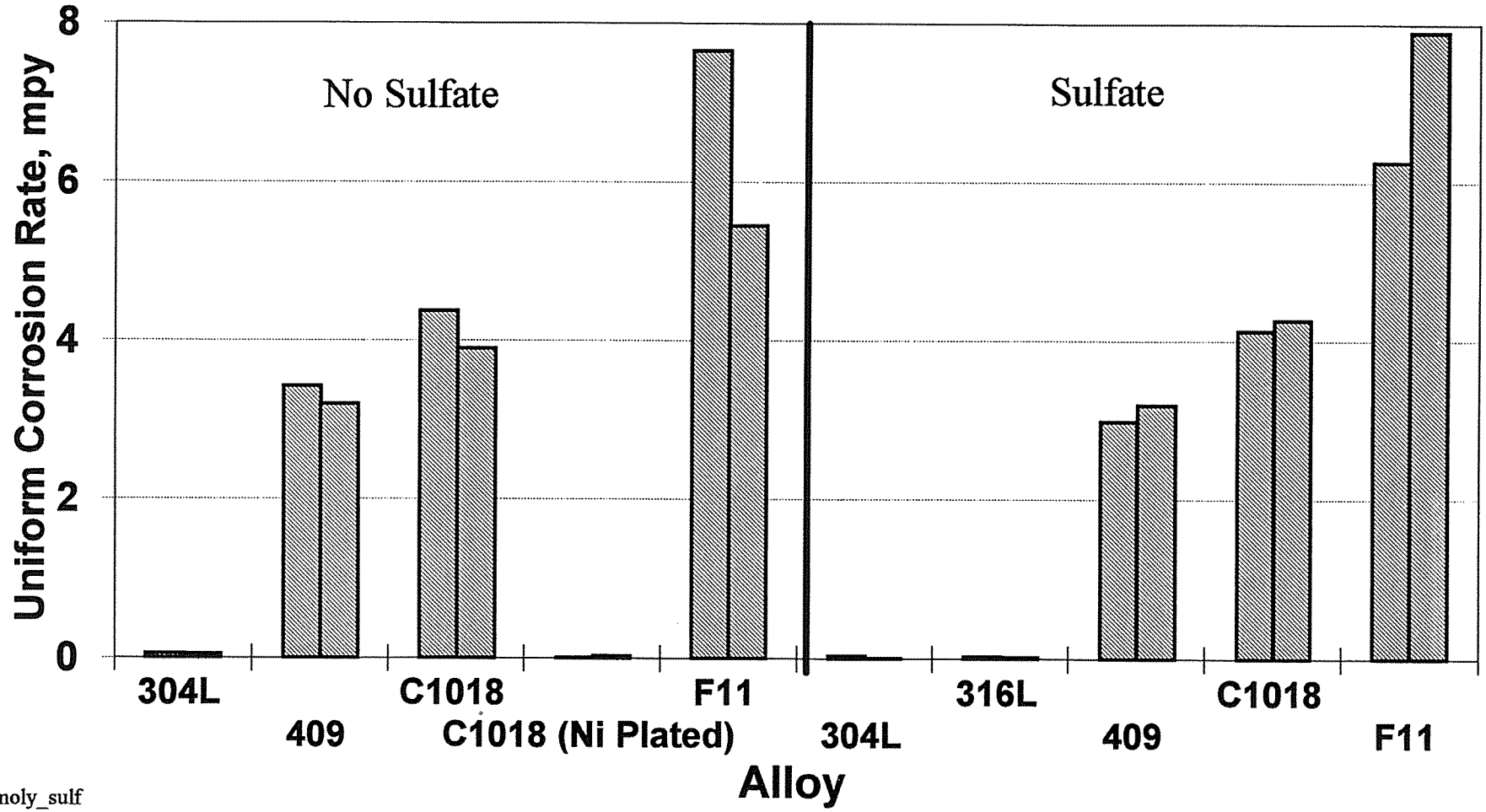

450F_moly_sulf

Figure 22. Corrosion rate results in molybdate inhibited solutions with and without sulfate, fully immersed flat coupons

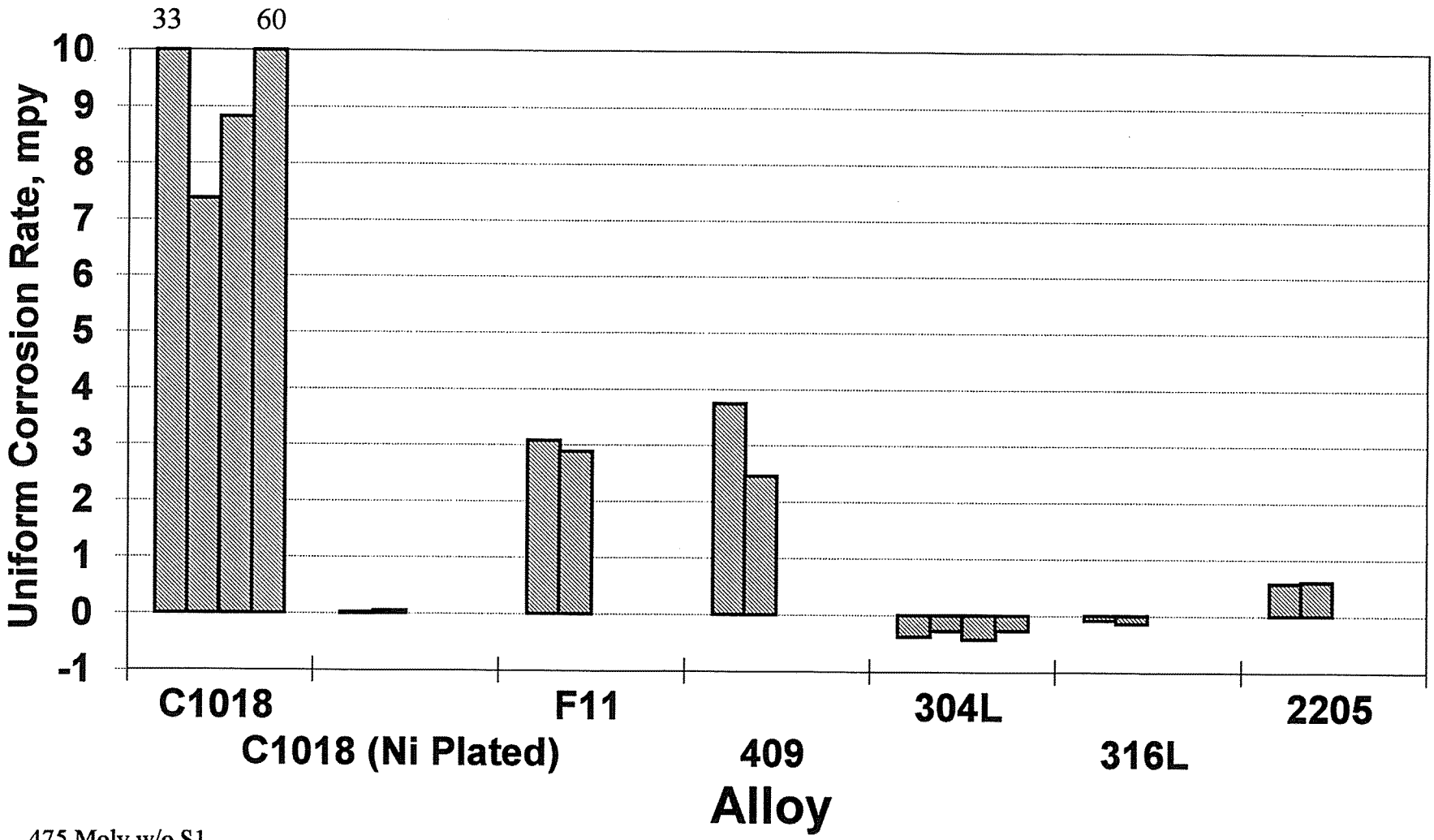

475 Moly w/o S1

Figure 23. Corrosion rate results in molybdate inhibited solutions at 475°F, fully immersed flat coupons

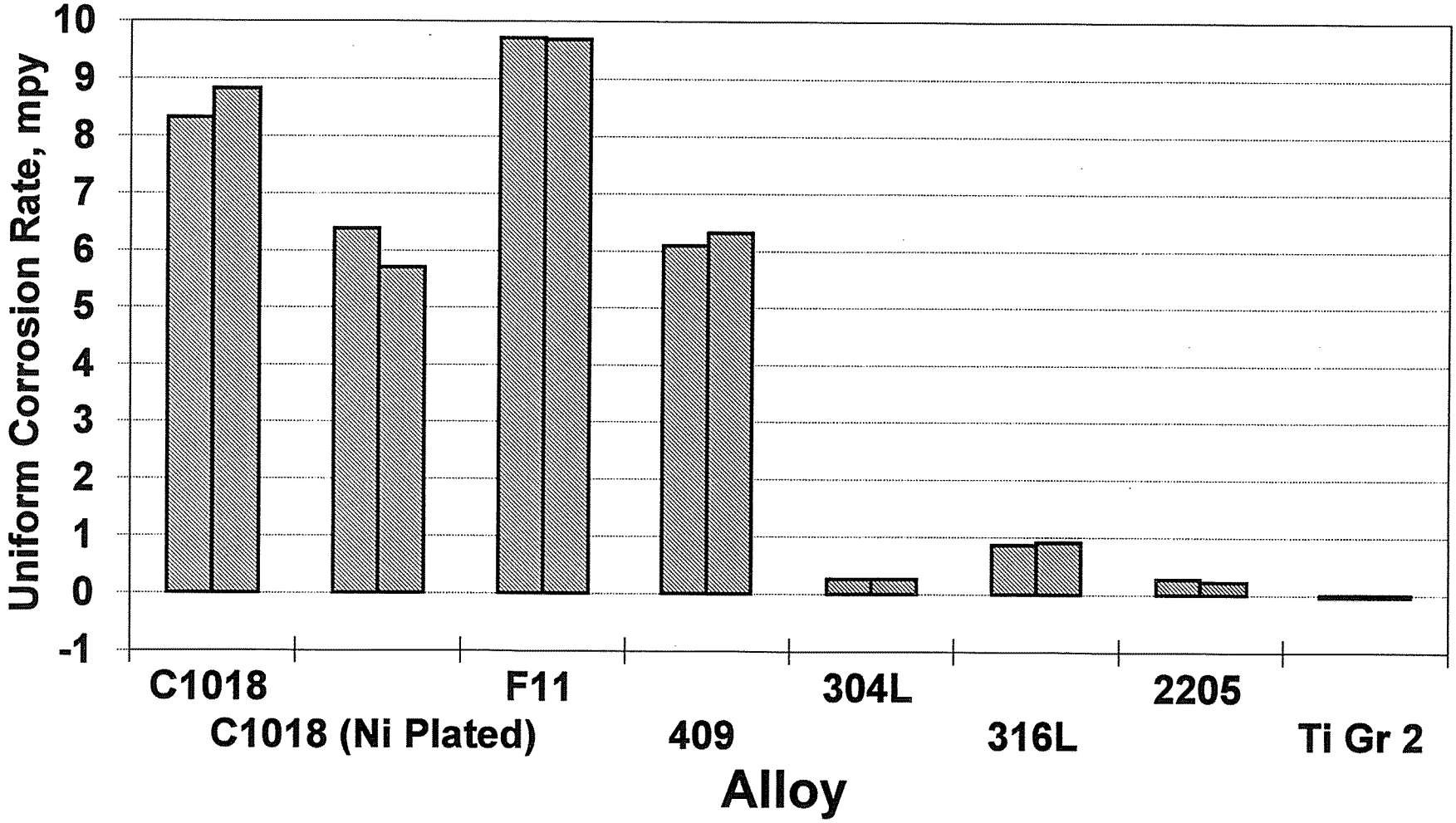

500 Moly w/o S

Figure 24. Corrosion rate results in molybdate inhibited solutions at 500°F, fully immersed flat coupons

Table 7. Corrosion Loop Materials Test Matrix

Inhibitor	Generator	Heat Exchanger
Molybdate	F11 (1.25Cr-0.5Mo)	SA179 (≈C1018)
Molybdate	410 (0.15C-1.0Mn-1.0Si-12Cr)	SA179 (≈C1018)
Silicate	F11 (1.25Cr-0.5Mo)	304L (18Cr-8Ni)
Molybdate	A-109 (≈C1018)	90Cu-10Ni

inhibitors in the four test loops is given in Table 7. The high cost of alloys such as 304, 316, and 2205 made them unattractive for use in a commercial product, especially if lower cost alloys might prove to be useful. Hence, the primary interest focused on C1018, F11, and 400 series stainless steels. Similarly, the previous use of molybdate as a corrosion inhibitor in commercially-available chillers focused attention on its use in the loop tests. Three of the corrosion loops were to use the molybdate inhibitor and one loop was reserved for the silicate inhibitor.

The choice of alloys for these tests was made only after considering cost, manufacturability, codes, and availability issues. Three sections of the ASME Boiler and Pressure Vessel Code were reviewed to determine the proper sections for rating the generator and the heat exchanger. York initially was concerned that Section 4 was the governing section for the generator, but Section 4 has an upper temperature limit of about 275°F, so it does not apply to generators operating at 450 to 500°F. Section 4 is a somewhat simplified version of Section 1, in that both sections deal with fired boilers, but Section 4 is widely used for small hot water heaters and boilers.

It was determined that Section 1 is the governing section for the generator because it covers fired boilers and pressure vessels and it has the appropriate temperature and pressure limits.

The heat exchanger clearly falls under Section 8, the section for unfired pressure vessels. Significantly, Section 8 allows the use of several stainless steels, including 304 and 304L.

The review determined that there were only two materials of real interest to York and Battelle for the fired generator. These are Grade 11 carbon steel, which was tested as F11, and alloy 405 stainless steel. No tests were conducted on 405, but tests were made on alloy 409, which is highly similar and newer. Significantly, 409 is not specifically allowed in Section 1 of the ASME Boiler and Pressure Vessel Code, nor is it generally available in any form except 2-inch tubing and sheet stock. Alloy 405 is more widely available and is allowed in Section 1. Grade 11 carbon steel is also allowed in Section 1 and is believed to be available in pipe and tubing. Both 405 and F11 require preheating of parts before welding, but neither alloy requires post-treatment of welds, which York viewed as more difficult. York is familiar with weld pretreatment in other applications, so they have the experience to evaluate these decisions. Difficulties in obtaining alloy 405 in the pipe sizes for a generator led to the final substitution of alloy 410 for one of the generators. A carbon steel alloy, A-109, was chosen for one generator in a molybdate-inhibited loop, to evaluate the lowest-cost steel available for heat-exchanger construction.

A high-quality carbon steel was chosen for two heat exchangers. The specific alloy is grade SA179, a carbon steel especially made for heat exchanger tubing. Its cost is only a little more than that of 1018 and similar alloys, but it is well suited to tubular heat-exchanger construction and use.

A 90-10 copper-nickel alloy was chosen as the material for one of the heat exchangers because this alloy had performed relatively well in the early test series and this alloy does not generate hydrogen gas as it corrodes, thus reducing the load on the purge system of the chiller.

Alloy 304L was chosen as one of the heat exchanger materials in a silicate-inhibitor test because it is an acceptable, familiar alloy that offers very low corrosion rates. It could be an excellent material for the tubes in a tube-in-shell heat exchanger. In this design, the concentrated solution going to the absorber would flow through the tubes but, because of the low corrosion rate for 304, very little gas would be generated to load the absorber purge system. The heat exchanger shell could be made of a lower cost alloy, such as Grade 11 or 1018, because the resultant gas could be trapped in the generator and condenser.

Corrosion Loop Construction

The corrosion test loops were assembled from components built in the Battelle absorption laboratory, using designs from a previous project.* The solution heat exchangers for these new tests were built to a larger capacity than used for the previous project by including one additional pass in the heat exchangers, for a total of seven passes in each exchanger. Each pass in the heat exchanger consisted of a tube-in-a-tube arrangement using 0.5-inch and 0.75-inch tubes having a wall thickness of 0.035 inch and an active length of 20 ft. The generators were constructed from 3-ft lengths of schedule 40 pipe.

A new and improved condenser design was utilized specifically for the higher temperature conditions of this project. The previous condenser design used four condenser tubes with parallel flow for the cooling water. This design gave low water flow rates in each tube and was believed to contribute to water side fowling. The new design used fewer tubes and series flow for the water flow. Figure 25 shows the schematic used for all of the corrosion loops. Components for all four loops were fabricated and three of the loops were completely assembled and tested. The fourth loop was partially assembled before its completion was deferred due to budget constraints.

---

* *Development of a Double-Effect Air-Conditioner Heater (DEACH)*, GRI-92/0205, Final Report, April 1992.

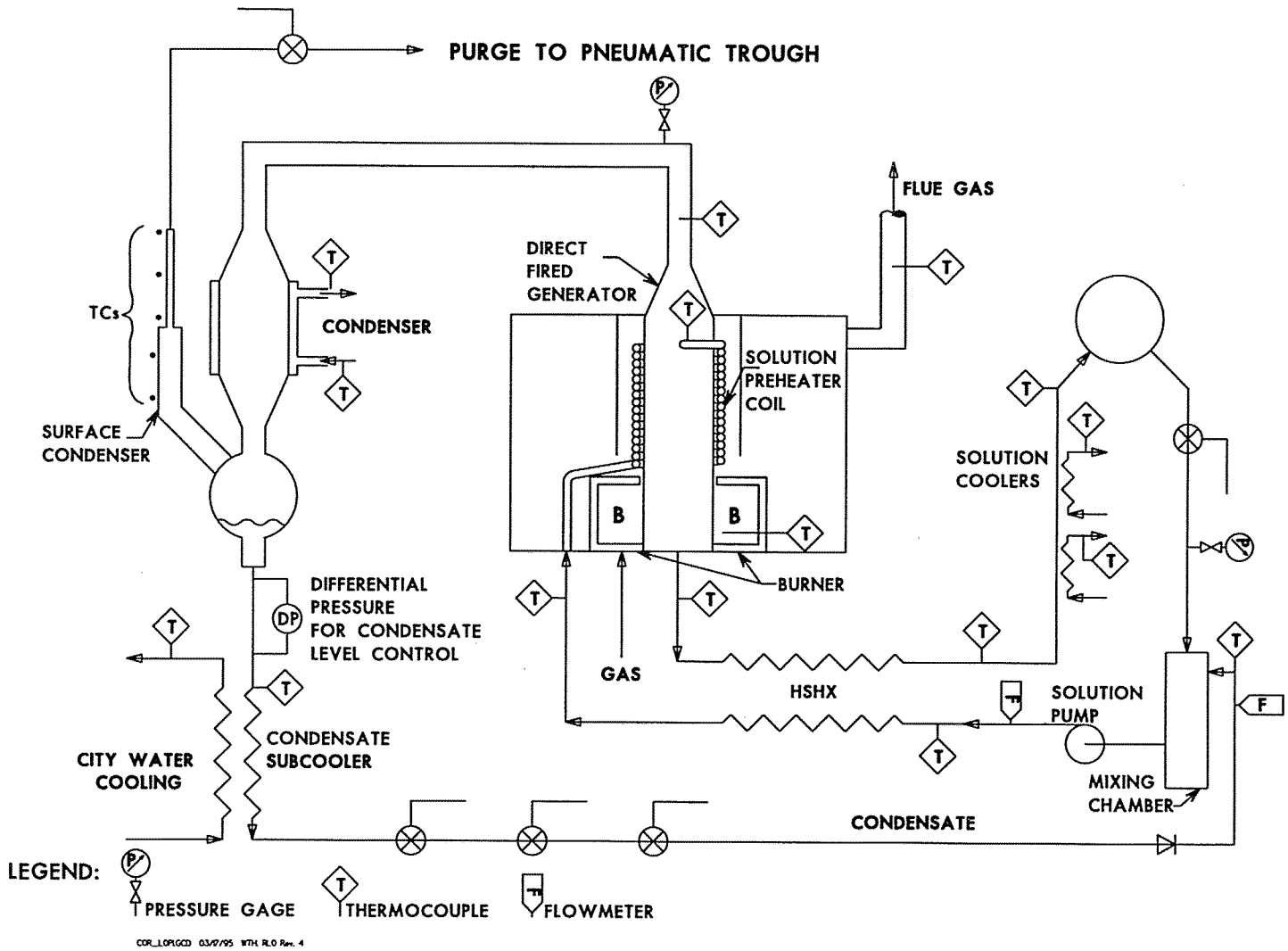

Figure 25. Schematic diagram for the corrosion test loops

Testing Results

The loops were charged with the molybdate inhibitor using the formulation provided by York as their preferred mixture for current production chillers.

The loops were intended for continuous operation, 24 hours per day for 7 days per week. In practice, each loop was operated for multi-day campaigns, but a full week of uninterrupted testing was never achieved. All the loops experienced a failure of a major test component within four days of cumulative testing. In addition, each loop experienced minor problems that required loop shutdowns for maintenance. The loops were operated under stable, open-loop control, with operator attention required only at intervals of up to 12 hours. The gas generation rate was manually measured at hourly intervals during early operations, and at longer intervals later in each test.

Figures 26 to 28 show the results of testing in the three loops. Figure 26 shows the results for loop 1, obtained in three test periods. The results for each test period are shown by the solid lines. The generator outlet temperature was in the 400 to 440°F range for all three test periods. Table A-1 gives the temperature for the generator solution outlet for each test along with the corresponding gas generation rate.

The first test period was terminated by a leak of solution from the loop. This leak was from a joint in the tubing connecting the generator outlet and the heat exchanger. This leak was repaired and testing was resumed. The second test period was terminated by a high pressure alarm on the generator, due to low cooling water flow of possible condenser fouling. The third test period was immediately begun, only to be terminated by the second leak. The second leak was from a pin-hole in the preheater coil inside the burner shell. Since this leak was hidden inside the shell it was not detectable until the loop lost enough solution to cause the pump to loose suction, resulting in a low flow rate alarm and a loop shutdown. The generator and preheater coil were disassembled to find the source of the

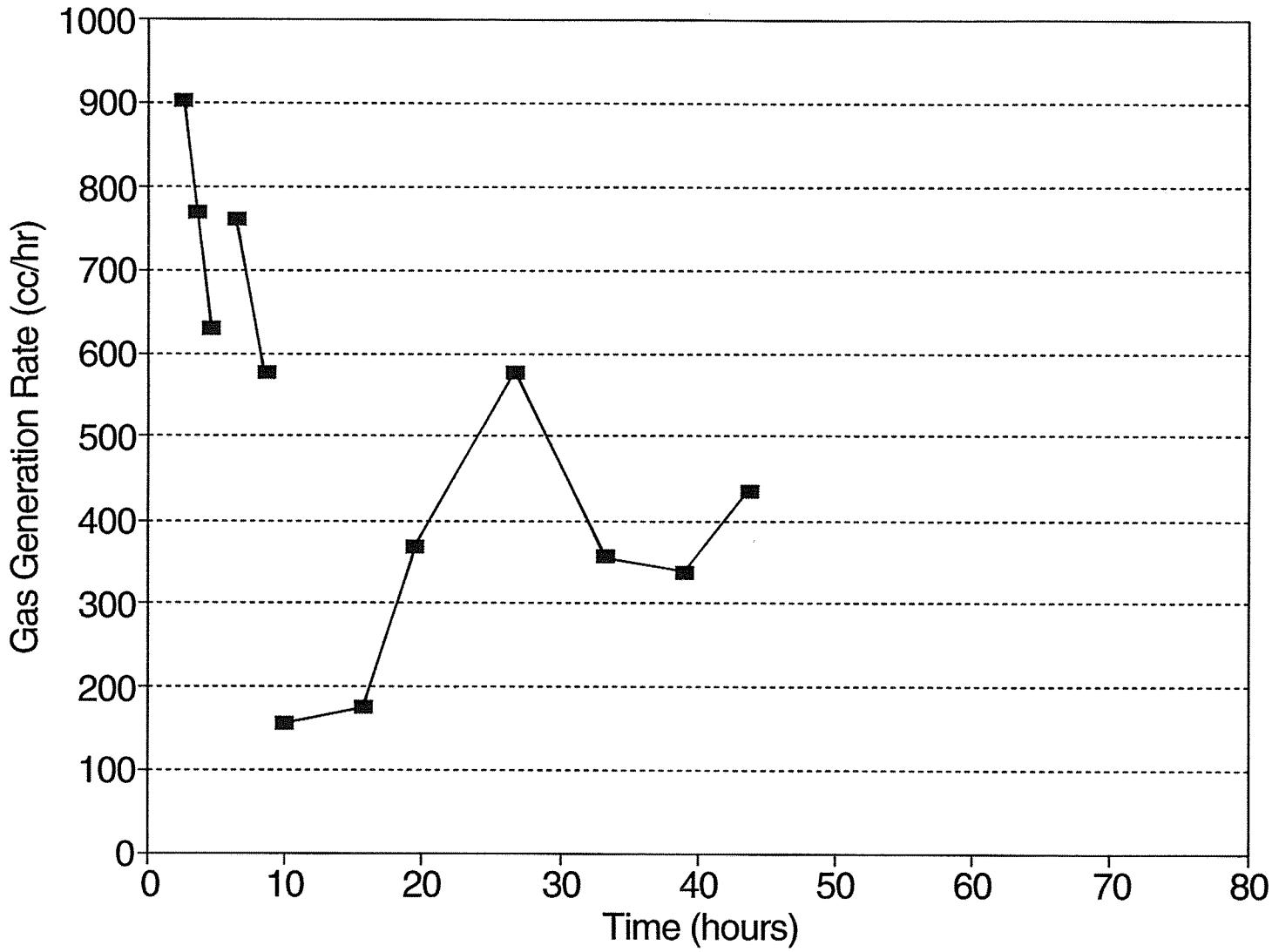

Figure 26. Gas generation rate for loop 1, F11 generator and SA 179 heat exchanger

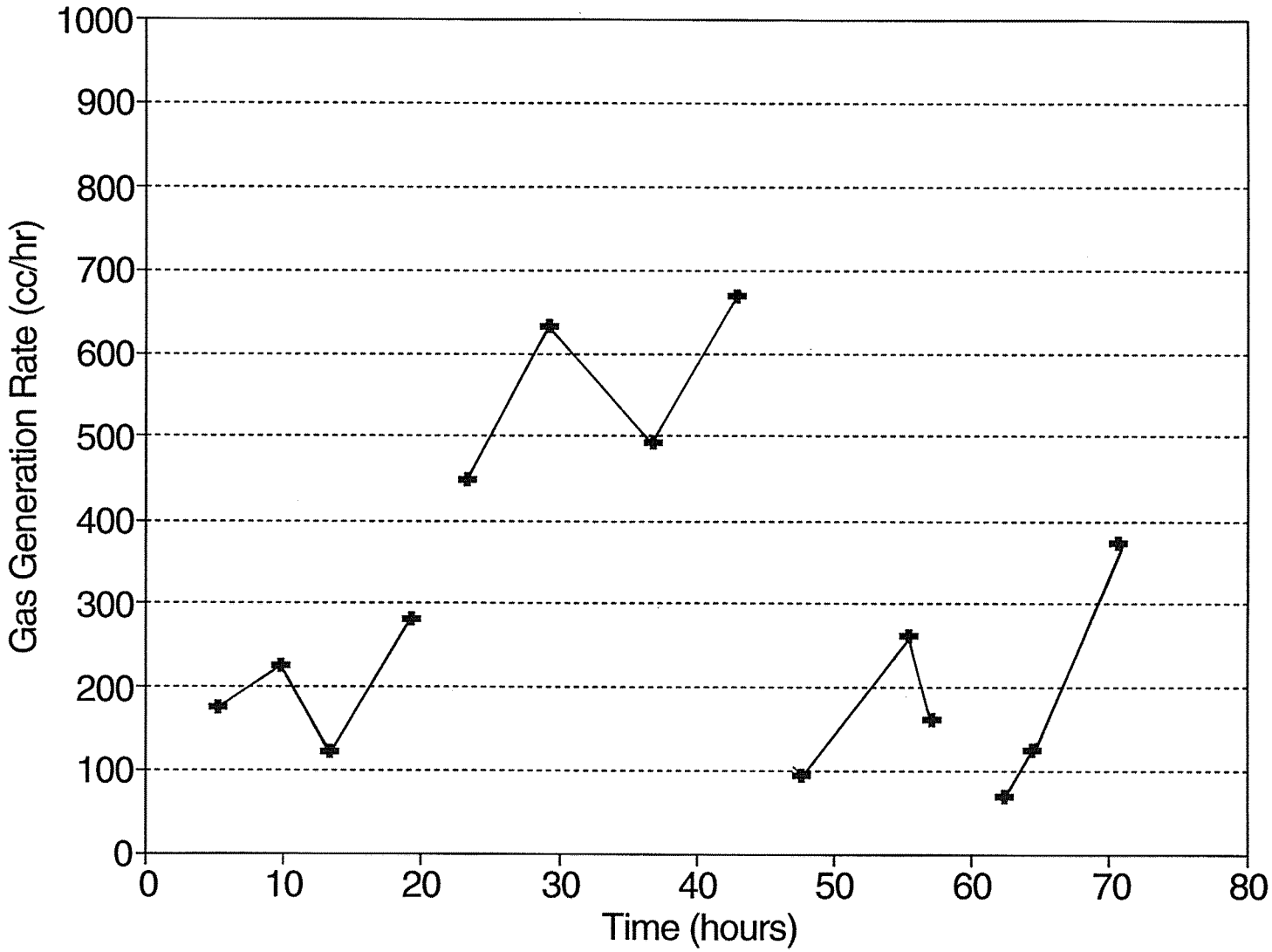

Figure 27. Gas generation rate for loop 2, 410 generator and SA 179 heat exchanger

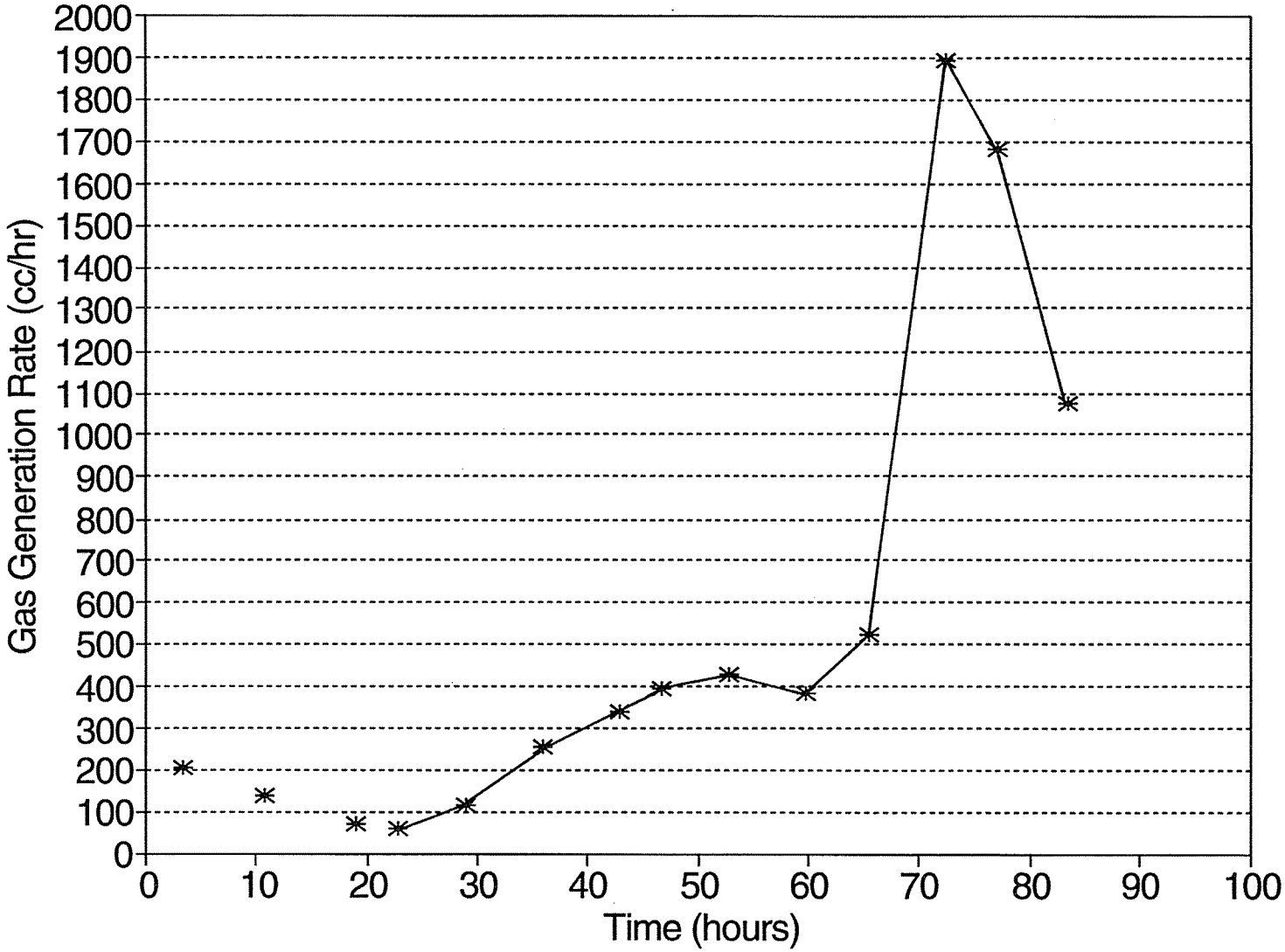

Figure 28. Gas generation rate for loop 3, A-109 generator and 90Cu-10Ni heat exchanger

leak. The leak was located in the first turn of the preheater coil, where the coil had one small area of contact with the gas shield. The gas shield is designed to direct the hot flue gas from the combustion chamber past the generator tube and away from the preheater coil. Thus, the gas shield operates at a very high temperature, probably 700 to 900°F. This one contact point exposed the coil to a localized high temperature and probably lead to a higher than average corrosion rate. The hole in the tube was of a conical shape, with the apex of the cone having breached the outer wall of the tube. The failed area of the precooler was sectioned and photographed (Figure A-6) for reference.

The gas generation rate was expected to decrease during a test, but these two values were significantly below expectation. The two lowest data points may be abnormally low because of gas leakage from the loop. The first point for the third test period was lower than expected, also possibly due to gas leakage.

Figure 27 shows the results for loop 2, obtained in three test periods. Again the data points for each test period are connected by a solid line. The three points recorded in the first 20 hours of testing show the results of testing at a peak generator temperature of less than 390°F. The remainder of the points were obtained at a generator temperature of 410 to 440°F. All other tests have shown generally decreasing gas generation rates during testing, in contrast to these test results.

These tests were terminated by a cracked weld in the generator. These tests showed an unusual pattern of rising gas generation rate during the test. The cracked area near the weld and the interior of the generator and heat exchanger were photographed (Figure A-7) for reference.

The testing of this loop was also interrupted twice by tubing leaks and the need to repair them. Both leaks were located at a joint in the line from the generator to the solution heat exchanger. This line had been sprayed with hot LiBr solution from the first leak in loop 1. The line had been cleaned immediately, but apparently the cleaning was not

able to prevent sufficient corrosion to cause these leaks. The entire line was replaced following the second leak in this joint and no further leaks developed in this line. Laboratory policy now requires a barrier wall between adjacent test loops and the replacement of all high temperature components that are exposed to solution spills.

Figure 28 shows the results for four test periods on loop 3. The presence of the copper alloy heat exchanger is clearly evident in the first three test periods. In contrast to the results from loop 1, which had a similar generator material but a carbon steel heat exchanger, the results for this first three test periods showed a much lower gas generation rate.

The first three tests were interrupted by minor component failures shortly after each test was begun. The first test was stopped to repair a joint leak in the tubing between the generator and the heat exchanger. The second and third tests were stopped by low flow alarms that were traced to pump failures. Two identical magnetic-drive gear pumps were used in these tests, and both failed by magnet decoupling. When the pumps were removed and disassembled copper particles were found in the gears. Manually turning the shaft of the pumps revealed a slight bind as the gears passed the copper particles. The precipitation of copper from low temperature solution was observed once before on another project.* It appears that the copper is dissolved into the solution at high temperature, building up to a concentration that is soluble only at the high temperature of the generator or heat exchanger. When the solution cools and passes through the absorber or pump, the copper concentration is above the saturation limit and copper particles appear in the solution. The resolution of this problem was to obtain a direct-drive gear pump and use a direct-current motor to set the proper speed for the required flow rate. The final test was conducted with this arrangement.

---

* *Development of the Dual-Cycle Absorption Heat Pump for Residential Application*, GRI-90/0075, Final Report, April 1990.

The fourth test period showed exceedingly high gas generation rates for the last 12 hours of the test when the loop operated at temperatures of 435 to 465°F. The gas generation rate for this test period was much higher than any rate measured in this laboratory. Clearly, the alloy A-109 generator was corroding much more rapidly than the F11 generator in loop 1. After a low flow rate alarm shut down this loop, a leak developed in the generator area, resulting in a loss of solution from the generator. The leak was found to be at a joint in the preheater coil, where two 20-ft pieces of tubing had been joined to makeup the required 40 feet of tubing for the coil. This leak (see Figure A-8) exposed the exterior of the generator to hot solution, terminating the test.

Conclusions

Additive Separation Evaluations

The additive separation efforts on this project did not lead to the clear identification of an apparently attractive means to enhance absorber performance in a chiller having a generator operating temperature in the 400 to 500°F range. Additive separation is intended to minimize the decomposition of the additive in the high temperature generator and thus maintain the enhanced performance that results from the absorber additive.

The separations tests conducted in this project led to the conclusion that additives such as 2EH probably cannot be economically separated from the $LiBr/H_2O$ solution by using gravimetric, thermal, or electroacoustic techniques. Part of the difficulty with the efforts to separate the 2EH from the solution is that the additive is partly dissolved in the solution and only partly mixed with the solution. The mixed portion may be separable by mechanical means, but removing the dissolved additive may require a chemical process.

The best alternatives may be to use only additives with high-temperature stability, to continue to use 2EH as the absorber additive and to replenish the 2EH charge when

high-load conditions occur, or are expected, or to develop and prove an alternative separation technique.

A stable, high-temperature additive, DFH, was tested in the absorber of a 40 RT chiller. These test results showed that DFH can make a technically significant improvement in absorber performance. However, this performance improvement is also significantly less than can be obtained with 2EH. Also, there are potentially significant chiller redesign and cost issues to be resolved before DFH can be considered a practical additive.

Materials Compatibility Evaluations

The materials compatibility efforts on this project showed the potential for using both molybdate and silicate as independent corrosion inhibitors in 450 to 500°F LiBr solutions. Both inhibitors are very effective when higher cost alloys such as 304L, 316L, and 2205 are considered. The silicate inhibitor showed potential for inhibiting stress-corrosion cracking in 304 and 316 stainless steels, a potentially significant finding.

Weight-loss coupon tests showed that lower cost alloys, such as F11, C1018, and 409, might resist the corrosive attack of the LIBr solution sufficiently to be of practical value. However, corrosion loop tests involving alloys A-109 (an alloy similar to C1018), F11, 410, and SA 179, showed high initial gas generation rates, especially as compared to purge system capacities that typify small-scale chillers. Alloy A-109 showed a particularly high gas generation rate at the nominal design temperatures of 435 to 465°F. Because the coupon tests cannot include the effects of solution flow and boiling heat transfer, as do the corrosion loop tests, the corrosion loop test results are expected to be less favorable than the coupon test results for any alloy. It is anticipated that the corrosion rates implied by the gas generation rates measured in the corrosion loop tests may require the reevaluation of the materials choices for a high-temperature chiller.

A cupro-nickel alloy, CDA706, was tested in one of the corrosion loops as a heat-exchanger material. Although this alloy cannot contribute to the gas generation rate, as it corrodes it does result in the saturation of the LiBr with copper. Since the copper can attain an equilibrium concentration at the peak cycle temperature, the copper can precipitate from the LiBr at the lower temperatures found in the pump and absorber. Thus, the high-temperature use of a cupro-nickel alloy may not be acceptable in a chiller because of precipitation issues.

Materials Recommendations

The following recommendations for generator and heat exchanger materials are made, based on Battelle's analysis of the project results, for consideration by ORNL and York for a construction of a High Temperature Chiller. The recommendations and the rationale for them are based upon the test results and an understanding of the overall response of the materials under test.

Generator Materials

The choice for the generator material is alloy F11, a low-alloy steel that performed better than either the 410 or the A-109 alloys.

The generator made of alloy A-109 gave the highest gas generation rate of any of the material combinations tested. The alloy A-109 generator was tested in a loop with a cupro-nickel heat exchanger, which does not contribute to the gas generation rate. Thus, all the gas generated in this loop must be attributed to the alloy A-109 generator, which had 2 ft^2 of wetted area. Whereas in the other loops, the larger, 60-ft^2 heat exchanger made a significant contribution to the gas generation. Thus, the conclusion that A-109 is greatly inferior to both alternatives tested even though the gas generation rates for the three loops are not so greatly different.

The generator made of alloy 410 produced gas generation rates comparable to the generator made of alloy F11, when both were tested with an SA 179 heat exchanger. The alloy 410 generator developed a crack at a weld, which caused the test loop to shut down, ending the test. The occurrence of the crack at a weld is the primary reason for not recommending the use of 410, or a similar 400 series alloy. Also the 400 series alloys were difficult to obtain in pipe and were costly.

The F11 alloy is recommended because it did not fail during the test and its gas generation rate was comparable to or lower than that for the 410/SA179 loop combination. Also, the gas generation rate decreased as the test continued, as expected. The coupon test results for this material showed a corrosion rate of 0.5 to 7 mils/year at 450°F with the molybdate inhibitor in 30-day tests, so the corrosion allowance must be carefully chosen. The corrosion loop containing the F11 generator also shut down due to a solution leak, but this leak was in a section of SA 179 tubing that was subjected to a hot spot.

Heat Exchanger Materials

The recommended material for the solution-to-solution heat exchanger is SA 179. This material was used without problem for the heat exchanger in two of the test loops. As noted above, there was a leak in an SA 179 tube at a local hot spot, but this tube was being used as a heat recovery solution preheater coil, which may not be a part of high temperature chiller.

The SA 179 alloy gave relatively trouble-free performance during the tests. There was difficulty making welded or brazed repairs to the heat exchanger after solution leaks had been discovered, but no special difficulty was experienced in welding clean material that had not been exposed to LiBr solution. In addition, the SA 179 cannot tolerate hot spots, so the design and construction must avoid their potential occurrence.

The alternative material tested was a 90-10 cupro-nickel alloy that gave mixed results. The corrosion reaction for copper alloys in LiBr solution does not generate hydrogen gas, so the gas generated in the A-109/ 90-10 test loop was due only to the generator corrosion. However, the copper alloy did corrode and elevate the level of copper in the LiBr solution. From previous experience it appears that the copper concentration can approach a level that characterizes equilibrium conditions at the peak solution temperature. At lower temperatures, typical of those in an absorber or solution pump, copper precipitates from the solution as elemental copper. Copper has appeared as a plating on steel parts and as copper particles suspended in the solution. If a solution pump can tolerate the possible deposition of copper, and if the corrosion rate of the copper nickel can be tolerated, then a cupro-nickel alloy might be acceptable. Copper chemistry in LiBr solutions is a complex issue, so the use of copper alloys at high temperature is not recommended at this time.

APPENDIX A.

PROJECT PHOTOGRAPHS AND SUPPLEMENTAL DATA

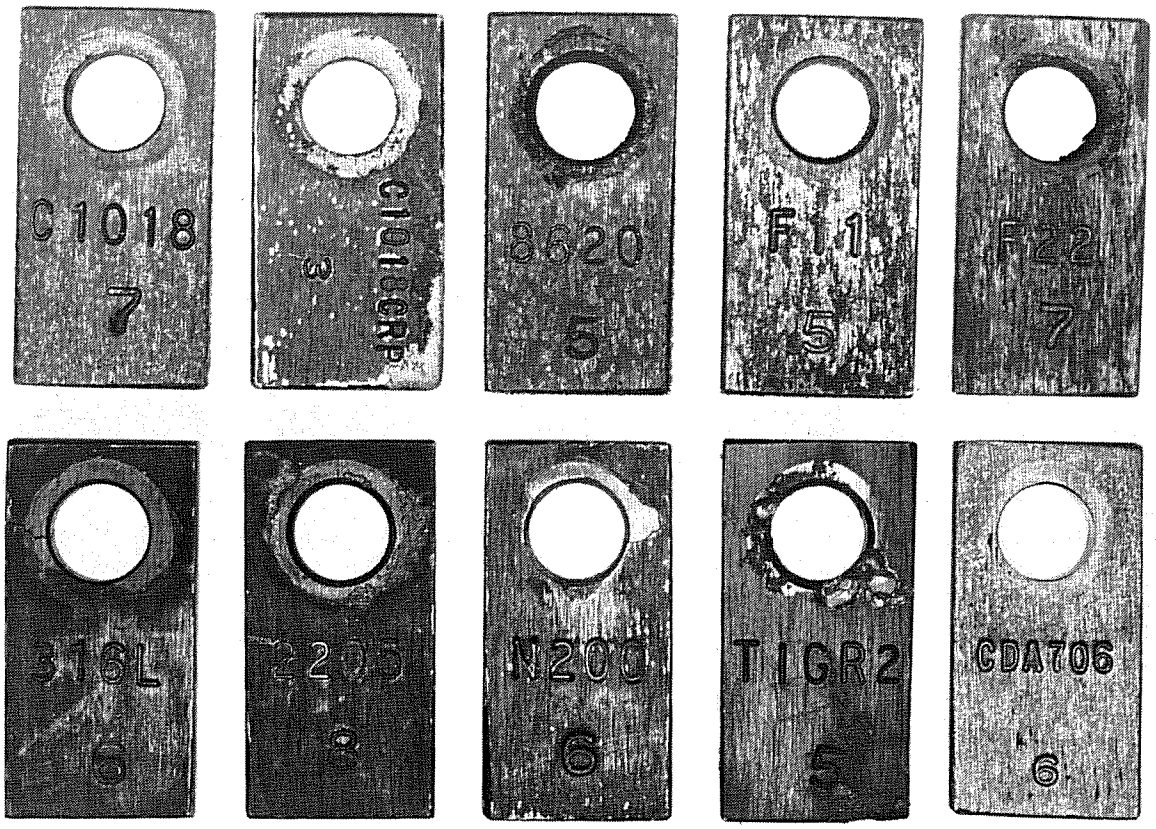

Figure A-1. Photograph of weight loss coupons, test series 1, fully immersed in chromate inhibitor, 450 °F, 32-day exposure

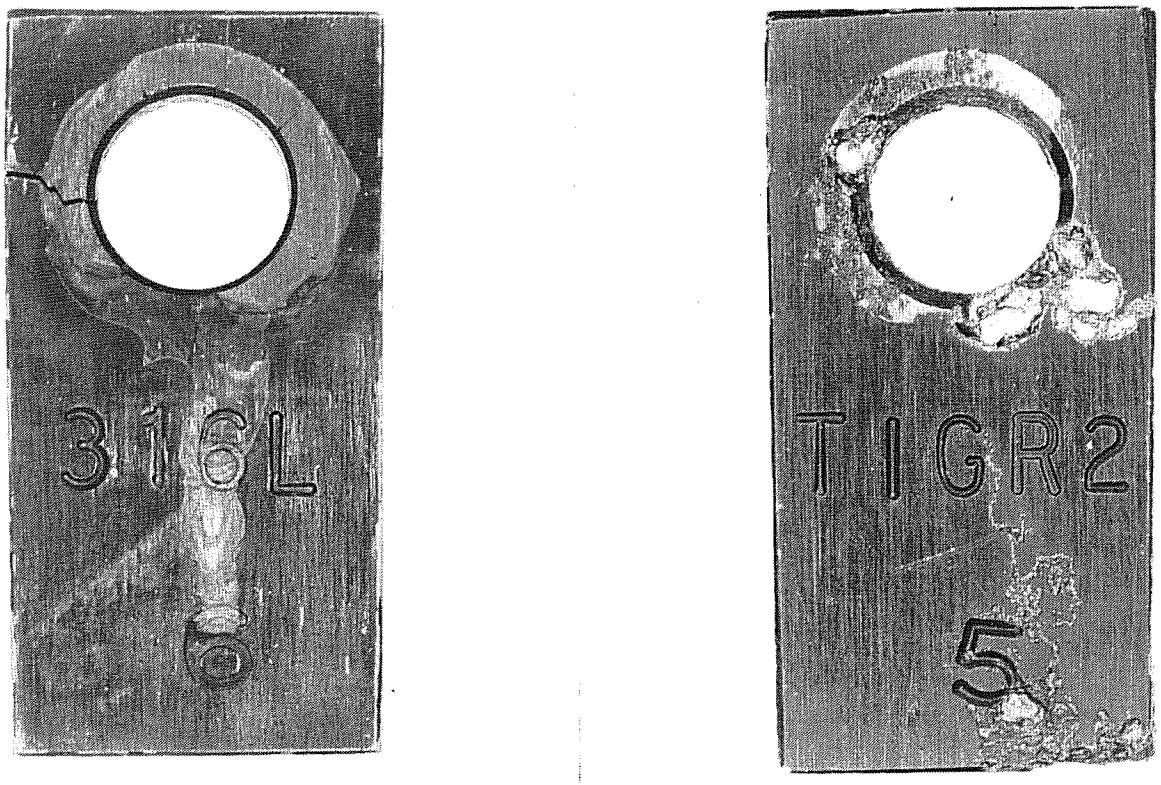

Figure A-2. Close-up photograph of 316L and TiGr2 weight loss coupons from Figure A-1, showing crack and pitting

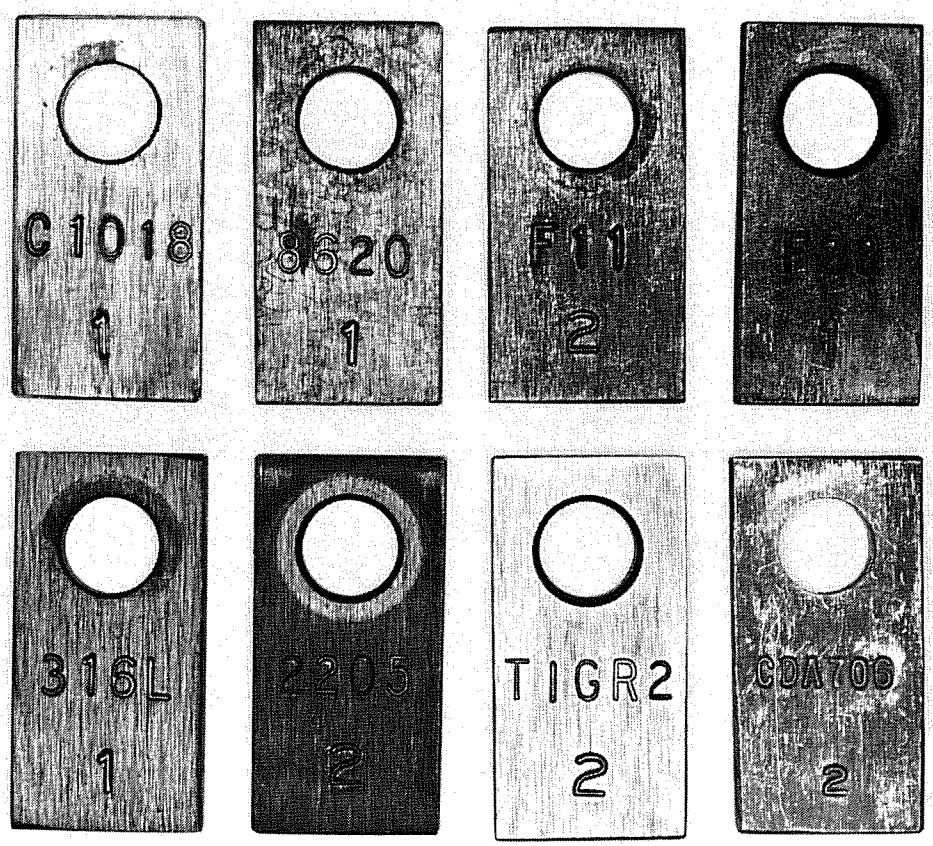

Figure A-3. Photograph of weight loss coupons, test series 1, fully immersed in molybdate inhibitor, 450 °F, 32-day exposure

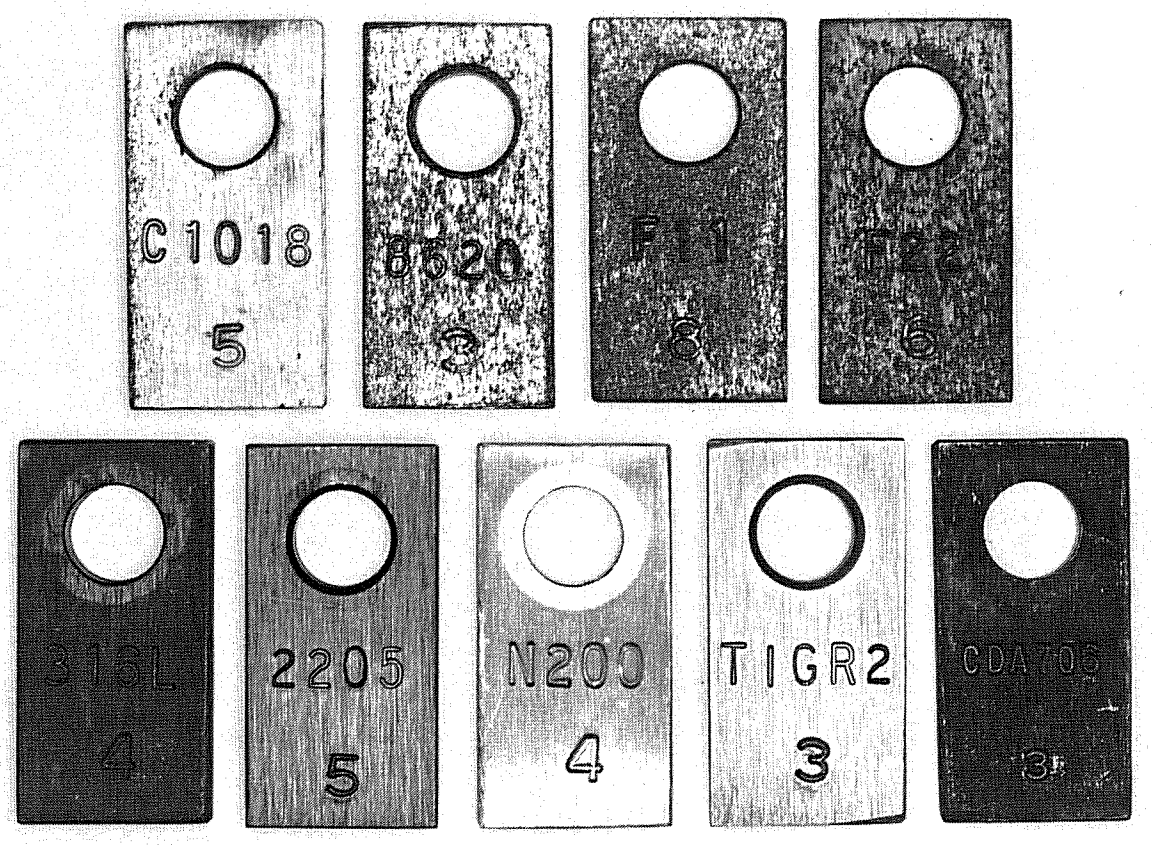

Figure A-4. Photograph of weight loss coupons, test series 1, fully immersed in silicate inhibitor, 450 °F, 32-day exposure

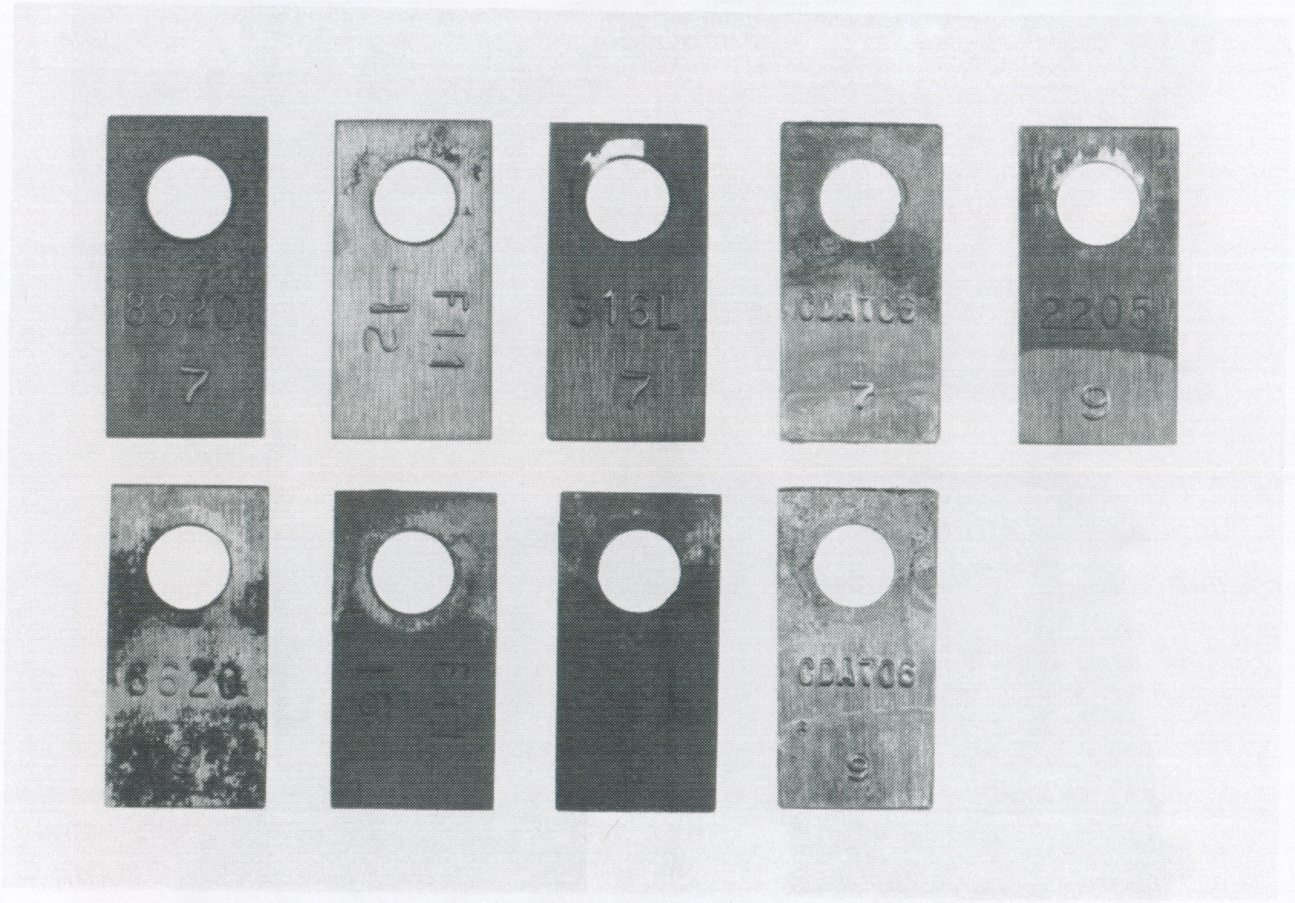

Figure A-5. Photograph of weight loss coupons, test series 1, partially immersed in silicate inhibitor (top row) or chromate inhibitor (bottom row), 450 °F, 32-day exposure

Figure A-6. Photographs of failed SA179 preheater tube, corrosion loop 1; top-tube after removal from loop; bottom-inside of tube after sectioning

Figure A-7. Photographs of sectioned components from corrosion loop 1; top-heat exchanger tubing (SA179), high-temperature end; bottom-generator shell (P11, pipe version of F11), lower end

Figure A-8. Photograph of cracked generator weld, fired zone, SS410 alloy, corrosion loop 2

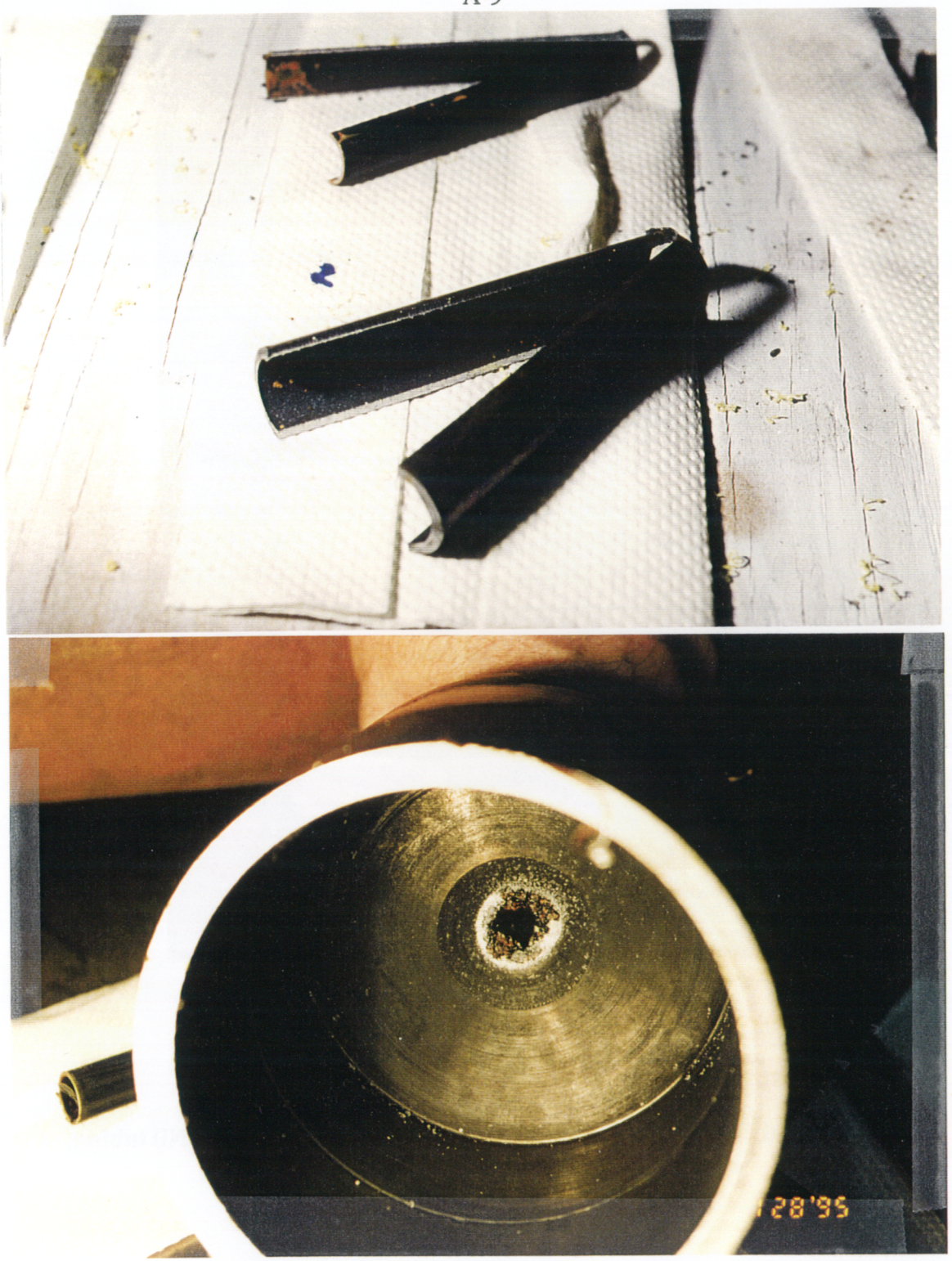

Figure A-9. Photographs of components from corrosion loop 2; top-heat exchanger tubing (SA179); bottom-generator shell, SS410

Figure A-10. Photograph of failed preheater coil joint (90Cu-10Ni) tubing, corrosion loop 3

Figure A-11. Photograph of section components from corrosion loop 3; top-heat exchanger tubing (90Cu-10Ni); bottom-generator shell (A109)

TABLE A-1. Gas Generation Rates and Corresponding Generator Solution Exit Temperatures

Loop 1		Loop 2		Loop 3	
Gas Generation Rate	Temperature	Gas Generation Rate	Temperature	Gas Generation Rate	Temperature
cc/hr	°F	cc/hr	°F	cc/hr	°F
904	400	175	380	202	340
770	390	225	390	138	410
630	390	123	390	70	440
760	410	282	400	57	370
575	410	447	430	115	370
155	430	633	430	255	370
173	412	494	420	341	405
367	430	669	440	392	405
577	430	95	390	428	410
356	420	262	420	382	405
336	425	160	410	526	455
434	420	69	440	1892	465
		125	430	1680	427
		373	420	1074	425